

LOCI OF TRIANGULAR ORBITS IN AN ELLIPTIC BILLIARD

DAN REZNIK, RONALDO GARCIA, AND JAIR KOILLER

ABSTRACT. We analyze the family of 3-periodic trajectories in an Elliptic Billiard. Taken as a continuum of rotating triangles, its Triangle Centers (Incenter, Barycenter, etc.) sweep remarkable loci: ellipses, circles, quartics, sextics, and even a stationary point. Here we present a systematic method to prove 29 out of the first 100 Centers listed in Clark Kimberling’s Encyclopedia are elliptic. We also derive conditions under which loci are algebraic. Finally, we informally describe a variety of delightful phenomena involving loci of orbit-derived centers and vertices.

Keywords: elliptic billiard, periodic trajectories, triangle center, derived triangle, locus, loci, algebraic.

MSC 51M04 and 37D50 and 51N20 and 51N35 and 68T20

1. INTRODUCTION

We’ve been interested in properties and invariants of the family of 3-periodics in the Elliptic Billiards (see Section 1.2). Because these are triangles we can analyze simple geometric objects derived from it. We were surprised [21] for example that this family (i) conserves the ratio of Inradius-to-Circumradius, (ii) maintains a special point (the *Mittenpunkt* [28]) fixed at the EB center [20, pl#03]¹, and that (iii) it can trace out a stationary circle [20, pl#04]. Surprisingly, some triangular invariants have been recently generalized to N -periodics (see [21, 1]).

This paper focuses on a related set of phenomena: the loci of *Triangle Centers* [12] such as the Incenter, Barycenter, etc., over the family of 3-periodic orbits. Constructions for a few basic centers and associated objects, appear in Figure 1.

An early result obtained from graphical simulation [20, pl#01] was that the locus of the Incenter was an ellipse², Figure 2, a fact subsequently proven [22]. This was quite unexpected since the map from orbit vertices to Incenter Cartesians is highly non-linear. Proofs soon followed for the ellipticity of both Barycenter [14] and Circumcenter [4, 6].

¹Videos will be cited herein as [20, pl#nn], where nn is its position on a playlist specially created.

²However, the locus of the Intouchpoints, which are the pedal points of the Incenter, was found not to be elliptic [20, pl#02].

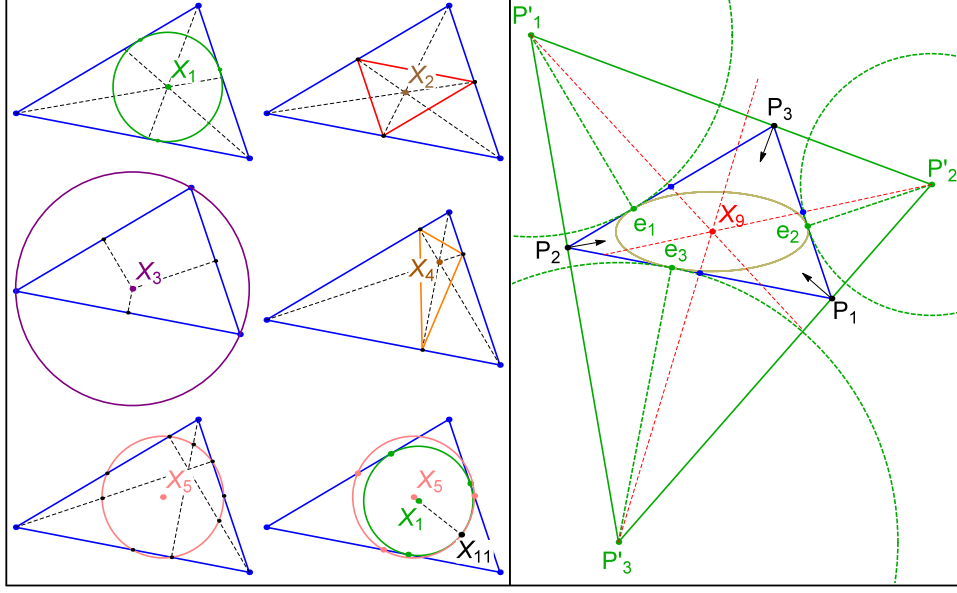


FIGURE 1. The construction of Basic Triangle Centers X_i , as listed in [12]. **Left:** The Incenter X_1 is the intersection of angular bisectors, and center of the Incircle (green), a circle tangent to the sides at three *Intouchpoints* (green dots), its radius is the *Inradius* r . The Barycenter X_2 is where lines drawn from the vertices to opposite sides' midpoints meet. Side midpoints define the *Medial Triangle* (red). The Circumcenter X_3 is the intersection of perpendicular bisectors, the center of the *Circumcircle* (purple) whose radius is the *Circumradius* R . The Orthocenter X_4 is where altitudes concur. Their feet define the *Orthic Triangle* (orange). X_5 is the center of the 9-Point (or Euler) Circle (pink): it passes through each side's midpoint, altitude feet, and Euler Points [28]. The Feuerbach Point X_{11} is the single point of contact between the Incircle and the 9-Point Circle. **Right:** given a reference triangle $P_1P_2P_3$ (blue), the *Excenters* $P'_1P'_2P'_3$ are pairwise intersections of lines through the P_i and perpendicular to the bisectors. This triad defines the *Excentral Triangle* (green). The *Excircles* (dashed green) are centered on the Excenters and are touch each side at an *Extouch Point* $e_i, i = 1, 2, 3$. Lines drawn from each Excenter through sides' midpoints (dashed red) concur at the *Mittenpunkt* X_9 . Also shown (brown) is the triangle's *Mandart Inellipse*, internally tangent to each side at the e_i , and centered on X_9 . This is identical to the $N = 3$ Caustic.

1.1. Summary of the Results. The aforementioned proofs draw upon tools from Algebraic and/or Analytic Geometry taking Triangle Centers on a case-by-case basis. Our main contribution here is an experimentally-guided (though rigorous) algorithm to quickly verify when any Triangle Center has an elliptic locus. We also show that when said centers are rational functions on the sidelengths, loci (elliptic or not) will be algebraic curves. Finally, we describe a variety of curious phenomena involving Triangle Centers and their loci.

This paper starts with a recap of our previous results, Section 2. Our main results appear in Sections 3 and 4. In the former we describe our new proof method apply it to the first 100 Triangle Centers in [12]. In the latter we provides conditions for a given locus to be algebraic.

In Section 5 we present a variety of loci phenomena which have delighted us and we hope delights the reader as well. We conclude in Section 6 with list of the videos mentioned in the paper and a few interesting questions. For convenience, longer calculations are placed in the Appendices.

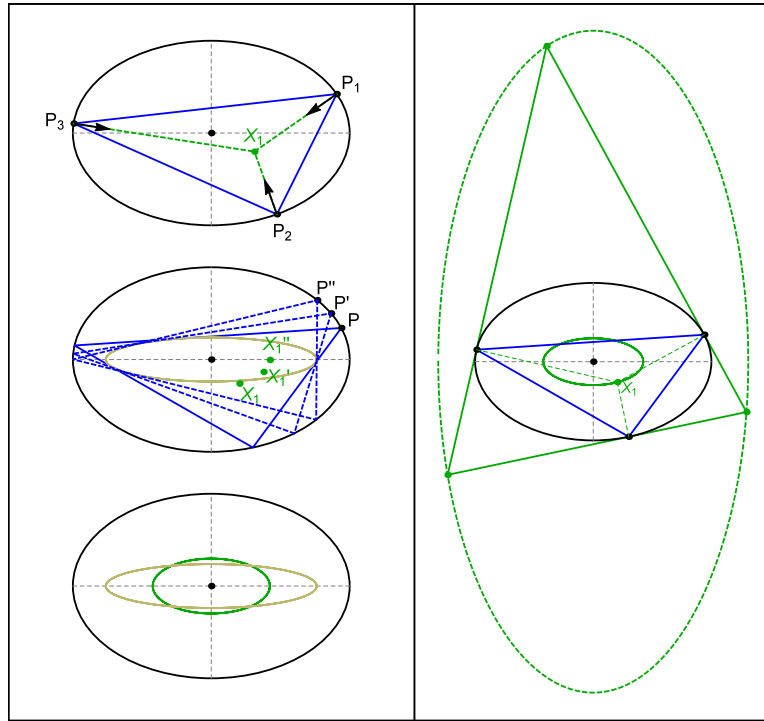


FIGURE 2. **Left Top:** A 3-periodic orbit, and its Incenter X_1 : where bisectors meet. **Left Mid:** Three triangular orbits, each identified by a starting vertex P, P', P'' , and their Incenters X_1, X_1', X_1'' . Also shown is the confocal Caustic (brown), the stationary *Mandart Inellipse* [28] of the 3-periodic family. **Left Bot:** the locus of X_1 over the 3-periodic family is an ellipse (green). Also shown is the Caustic (brown). **Right:** the Excentral Triangle (green) of a 3-periodic orbit (blue). The locus of its vertices (the Excenters) is an ellipse (dashed green) similar to a perpendicular copy of the locus of the Incenter (solid green inside the EB). This is the stationary *MacBeath Circumellipse* of the Excentral Triangle [28], centered on the latter's X_6 (i.e., the orbit's X_9) **Video:**[20, pl#01].

1.2. Review: Elliptic Billiards. Consider the ellipse \mathcal{E} with positive axes a, b :

$$(1) \quad f(x, y) = \left(\frac{x}{a}\right)^2 + \left(\frac{y}{b}\right)^2 = 1.$$

An Elliptic Billiard (EB) is a particle moving with constant velocity in the interior of \mathcal{E} , undergoing elastic collisions against its boundary [26, 23], Figure 3. For any boundary location, a given exit angle (e.g., measured from the normal) may give rise to either a quasi-periodic (never closes) or N -periodic trajectory [26], where N is the number of bounces before the particle returns to its starting location.

The EB is the only known *integrable* Billiard in the plane [10]. It satisfies two important integrals of motion: (i) Energy, since particle velocity has constant modulus and bounces are elastic, and (ii) Joachimsthal's, implying that all trajectory segments are tangent to a confocal Caustic [26]. The EB is a special case of *Poncelet's Porism* [3]: if one N -periodic trajectory can be found departing from some boundary point, any other such point will initiate an N -periodic, i.e., a 1d *family* of such orbits will exist. A striking consequence of Integrability is that for a given N , all N -periodics have the same perimeter [26].

2. RECAP OF PREVIOUS RESULTS

Kimberling [12] has classified thousands of Triangle Centers which he identifies by the X_i acronym: X_1 for Incenter, X_2 for Barycenter, etc. Conveniently, *Trilinear Coordinates* for each center are also provided [11], from which Cartesians can be obtained, see Appendix A.

Already established is the fact that the loci of Incenter X_1 , Barycenter X_2 and Circumcenter X_3 are ellipses [22, 4, 24, 6]. Below we show that the locus of the Orthocenter X_4 and of the 9-Point Circle³ Center X_5 are also elliptic, Figure 4 (left).

We also previously found that the locus of the Feuerbach Point X_{11} coincides with the Caustic and that of its Anticomplement⁴ X_{100} coincides with the EB. These phenomena appear on Figure 4 (right), and are viewable in [20, pl#07].

³Also known as the *Euler Circle*.

⁴Double-length reflection about the Centroid X_2 .

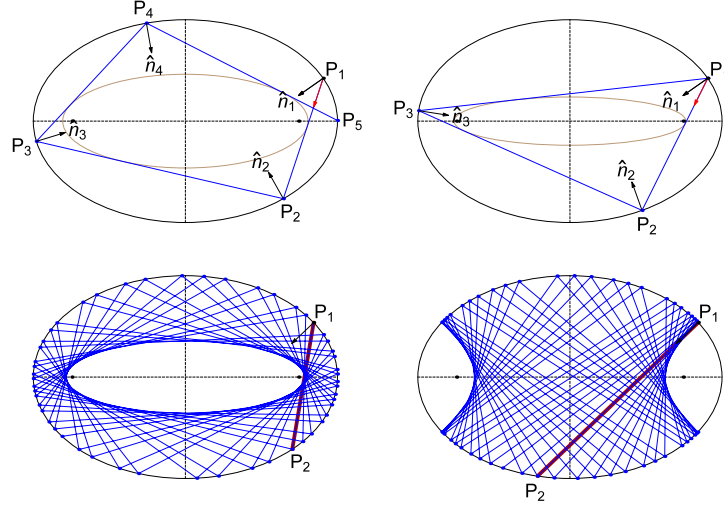


FIGURE 3. Trajectory regimes in an Elliptic Billiard. **Top left:** first four segments of a trajectory departing at P_1 and toward P_2 , bouncing at $P_i, i = 2, 3, 4$. At each bounce the normal \hat{n}_i bisects incoming and outgoing segments. Joachimsthal's integral [26] means all segments are tangent to a confocal *Caustic* (brown). **Top right:** a 3-periodic trajectory. All 3-periodics in this Billiard will be tangent to a special confocal Caustic (brown). **Bottom:** first 50 segments of a non-periodic trajectory starting at P_1 and directed toward P_2 . Segments are tangent to a confocal ellipse (left) or hyperbola (right). The former (resp. latter) occurs if P_1P_2 passes outside (resp. between) the EB's foci (black dots).

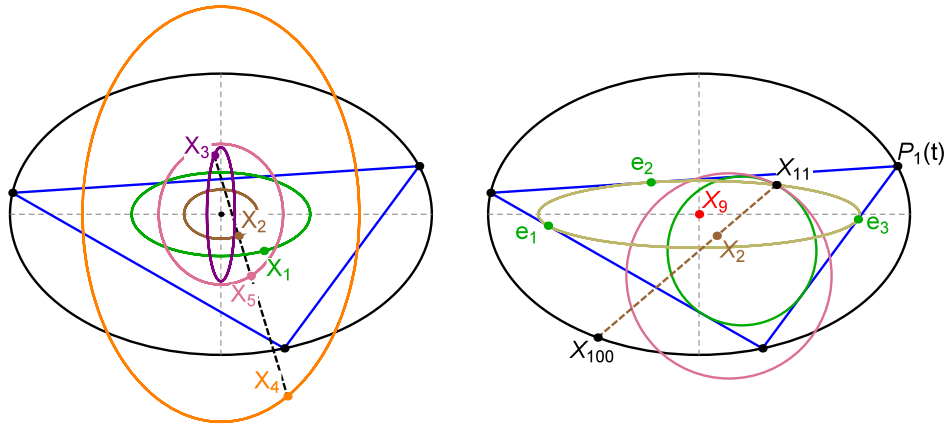


FIGURE 4. **Left:** The loci of Incenter X_1 , Barycenter X_2 , Circumcenter X_3 , Orthocenter X_4 , and Center of the 9-Point Circle X_5 are all ellipses, [Video \[20, pl#05\]](#). Also shown is the *Euler Line* (dashed black) which for any triangle, passes through all of $X_i, i = 1 \dots 5$ [28]. **Right:** A 3-periodic orbit starting at $P_1(t)$ is shown (blue). The locus of X_{11} , where the Incircle (green) and 9-Point Circle (pink) meet, is the Caustic (brown), also swept by the Extouchpoints e_i . X_{100} (double-length reflection of X_{11} about X_2) is the EB. **Video:** [20, pl#07].

A *Derived Triangle* is one obtained from the vertices of a reference one, in our case, the 3-periodic family. The following facts are known about them:

- the *Intouchpoints*’, vertices of the Intouch or Contact Triangle, sweep a locus with two self-intersections [21] (see Figure 5), [20, pl#02].
- the *Excenters*, vertices of the Excentral Triangle, sweep an Ellipse similar to a rotated copy of the X_1 locus [6], Figure 2, and viewable in [20, pl#06].
- the *Extouchpoints* sweep the Caustic [21], a result we prove below.

The are illustrated in Figure 5, and animated in [20, pl#09].

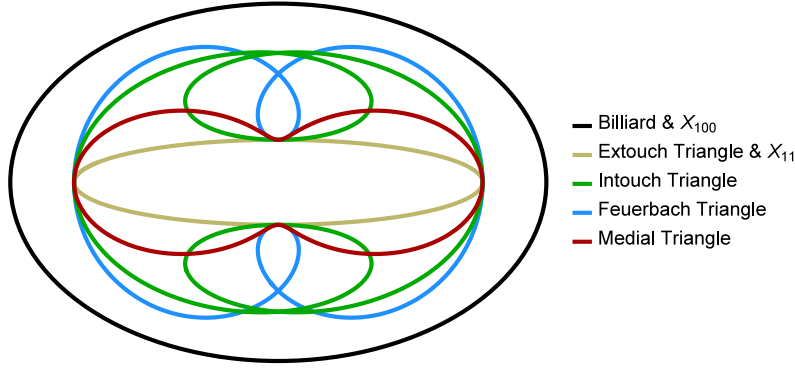


FIGURE 5. The vertices of the Intouch (green), Feuerbach (blue), and Medial (red) Triangles produce non-elliptic loci. Surprisingly, the Extouchpoints as well as the Feuerbach Point X_{11} (both shown brown), are identical to the $N = 3$ Caustic. Video [20, pl#07]

3. MAIN RESULT #1: 29 OUT OF FIRST 100 TRIANGLE CENTERS HAVE ELLIPTIC LOCI

Though a theory is still lacking for what governs the degree of the locus of a Triangle Center, a numerically-assisted (though rigorous) proof, explained below, allows us to state:

Theorem 1. *Out of the first 100 centers in [12], exactly 29 produce elliptic loci, all of which are concentric and axis-aligned with the EB. These are $X_i, i=1, 2, 3, 4, 5, 7, 8, 10, 11, 12, 20, 21, 35, 36, 40, 46, 55, 57, 63, 65, 72, 78, 79, 80, 84, 88, 90$. Specifically:*

- The loci of $X_i, i = 2, 7, 57, 63$ are ellipses similar to the EB.
- The loci of $X_i, i = 4, 10, 40$ are ellipses similar to a 90° -rotated copy of the EB.
- The loci of $X_i, i = 88, 100$ are ellipses identical to the EB⁵.
- The loci of X_{55} is an ellipse similar to the $N = 3$ Caustic.

⁵See below for more centers on the EB discovered by Peter Moses and Deko Dekov.

- The loci of $X_i, i = 3, 84$ are ellipses similar to a 90° -rotated copy of the $N = 3$ Caustic.
- The locus of X_{11} is an ellipse identical to the $N = 3$ Caustic.

The properties above are summarized in Table 1. Explicit expressions for the semi-axes in terms of a, b for the above appear in Appendix C.

| row | center | definition | similarity |
|-----|-----------|---|------------|
| 1 | X_1 | Incenter | J^t |
| 2 | X_2 | Centroid | B |
| 3 | X_3 | Circumcenter | C^t |
| 4 | X_4 | Orthocenter | B^t |
| 5 | X_5 | 9-Point Center | |
| 6 | X_7 | Gergonne Point | B |
| 7 | X_8 | Nagel Point | |
| 8 | X_{10} | Spieker Center | B^t |
| 9 | X_{11} | Feuerbach Point | C^+ |
| 10 | X_{12} | $\{X_1, X_5\}$ -Harm. Conjug. of X_{11} | |
| 11 | X_{20} | de Longchamps Point | |
| 12 | X_{21} | Schiffler Point | |
| 13 | X_{35} | $\{X_1, X_3\}$ -Harm. Conjug. of X_{36} | |
| 14 | X_{36} | Inverse-in-Circumcircle of X_1 | |
| 15 | X_{40} | Bevan Point | B^t |
| 16 | X_{46} | X_4 -Ceva Conjug. of X_1 | |
| 17 | X_{55} | Insimilicenter(Circumc., Incircle) | C |
| 18 | X_{56} | Exsimilicenter(Circumc., Incircle) | |
| 19 | X_{57} | Isogonal Conjug. of X_9 | B |
| 20 | X_{63} | Isogonal Conjug. of X_{19} | B |
| 21 | X_{65} | Intouch Triangle's X_4 | |
| 22 | X_{72} | Isogonal Conjug. of X_{28} | J |
| 23 | X_{78} | Isogonal Conjug. of X_{34} | |
| 24 | X_{79} | Isogonal Conjug. of X_{35} | |
| 25 | X_{80} | Reflection of X_1 about X_{11} | J^t |
| 26 | X_{84} | Isogonal Conjug. of X_{40} | C^t |
| 27 | X_{88} | Isogonal Conjug. of X_{44} | B^+ |
| 28 | X_{90} | X_3 -Cross Conjug. of X_1 | |
| 29 | X_{100} | Anticomplement of X_{11} | B^+ |

TABLE 1. The 29 Kimberling centers within X_1 to X_{100} with elliptic loci. Under “similarity”, letters B,C,J indicate the locus is similar to EB, Caustic, or Excentral locus, respectively. An additional + (resp. t) exponent indicates the locus is identical (resp. similar to a perpendicular copy) to the indicated ellipse. Note: the ellipticity of $X_i, i = 1, 2, 3, 4$ was previously proven [22, 27, 4, 6].

Aside from X_{88} and X_{100} an extra 27 Triangle Centers which also lie on the EB [12, X(9)] have been discovered by Peter Moses⁶. The same author also lists 57 Triangle Centers whose *isotomic conjugates* [28] lie on the EB, a fact co-discovered in [8]. An animation of the first Moses list is viewable in [20, pl#10].

3.1. Proof Method.

(1) Select Candidates

- Let the EB have axes a, b such that $a > b > 0$. Calculate $P_1(t_k) = (a \cos(t_k), b \sin(t_k))$, for M equally-spaced samples $t_k \in [0, 2\pi)$, $k = 1, 2, \dots, M$.
- Obtain the Cartesian coordinates for the orbit vertices $P_2(t_k)$ and $P_3(t_k)$, $\forall k$ (Appendix B.2).
- Obtain the Cartesians for Triangle Center X_i from its Trilinears (Appendix A) for $\forall t_k$. Note: if analyzing a derived triangle's vertex, convert a row of its *Trilinear Matrix* to Cartesians (Appendix A).
- Least-squares fit an origin-centered, axis-aligned ellipse (2 parameters) to the $X_i(t_k)$ samples. Accept the locus as potentially elliptic if the numeric fit error is negligible⁷, rejecting it otherwise (see below for a discussion on false negatives).

(2) Verify Ellipticity Algebraically:

- Taking a, b as symbolic variables, calculate $X_i(0)$ (resp. $X(\pi/2)$), placing P_1 at the right (resp. top) EB vertex. The orbit will be a sideways (resp. upright) isosceles triangle, Figure 6. By Lemma 2, X_i will fall along the axis of symmetry of either isosceles.
- The x coordinate of $X_i(0)$ (resp. the y of $X_i(\pi/2)$) will be a symbolic expressions in a, b . Use them as candidates for semiaxis lengths a_i, b_i .
- Taking t also as a symbolic variable, use a computer algebra system (CAS) to verify if $X_i(t) = (x_i(t), y_i(t))$, as parametrics on t , satisfy $(x_i(t)/a_i)^2 + (y_i(t)/b_i)^2 = 1$, $\forall t$.
- If the above is true, and since $X_i(t)$ is guaranteed to cover the entire ellipse (Lemma 2 below), assert that the locus of X_i is an ellipse⁸

Robust fitting of ellipses to a cloud of points is not new [25, 5]. In our case, the only source of error in Triangle Center coordinates is numerical precision, whose propagation can be bounded by Interval Analysis [15]. Therefore false

⁶Moses lists centers as lying on the so-called X_9 -centered Circumellipse (independent of Billiards). As X_9 is stationary for the 3-periodic family [21], Moses' points imply these will be on the EB.

⁷In our experiments we found it unnecessary to recheck the fit error for other values of a, b .

⁸Note: If analyzing a derived triangle vertex, use Lemma 3.

negatives in the detection process are ruled out. As an emblematic case, consider X_6 . In Section 5.6 its locus is shown to be a quartic. At $a/b = 1.5$ it is visually indistinguishable from an ellipse. However, its fit error is 10-20 orders of magnitude higher than the ones produced by true elliptic loci.

3.2. Locus Coverage of Ellipse.

Lemma 1. *A triangle center X_i of an isosceles triangle is contained in the axis of symmetry of the triangle, Figure 6.*

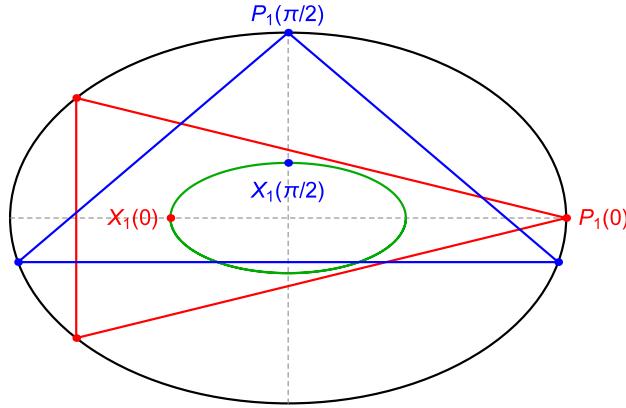


FIGURE 6. When P_1 is placed on the right (resp. top) vertex of the EB, the orbit is a sideways (resp. upright) isosceles triangle, solid red (resp. solid blue). Also shown (green) is the locus of a sample Triangle Center, e.g., X_1 . Lemma 2 shows that when a triangle is isosceles, all of its Triangle Centers will lie on the axis of symmetry. Notice how $X_1(0)$ (resp. $X_1(\pi/2)$) lies on the major (resp. minor) axis of the EB.

Proof. Consider an isosceles triangle with vertices $P_1 = (a_1, 0)$, $P_2 = (-b_1, c_1)$ and $P_3 = (-b_1, -c_1)$ having axis of symmetry the axis x . Let X_i have Trilinears $x : y : z$. Its Cartesians are given by Equation (3). As $s_2 = s_3$ and h is symmetric on its last two variables $h(a, b, c) = h(a, c, b)$ it follows that $y_i = 0$. \square

Lemma 2. *If the Cartesian parametric for a Triangle Center X_i can be shown to satisfy the equation of an axis-aligned ellipse, then its locus over the 3-periodic family will cover said ellipse, Figure 7.*

Proof. The family of 3-periodic billiard orbits contains four isosceles triangles. Therefore, for $P_1(t) = (a \cos t, b \sin t)$ it follows that $X_i(0) = (\pm a_i, 0)$, $X_i(\pi/2) = (0, \pm b_i)$, $X_i(\pi) = (\mp a_i, 0)$ and $X_i(3\pi/2) = (0, \mp b_i)$. Therefore, when $P_1(t)$ travel an arc of ellipse, say $\text{arc}((a, 0), (0, b))$, the locus $X_i(t)$ will go through one of the arcs $\text{arc}((\pm a_i, 0), (0, \pm b_i))$. Applying the Theorem of the Intermediate Value [16, Chapter 1, page 38], it follows that when the loci of points X_i is on an axis-aligned ellipse, they cover the said ellipse. \square

Lemma 3. *If the Cartesian parametric for the vertex of an orbit-derived triangle (i.e., a row in its trilinear matrix) can be shown to satisfy the equation of an axis-aligned ellipse, then its locus over the 3-periodic family will cover it.*

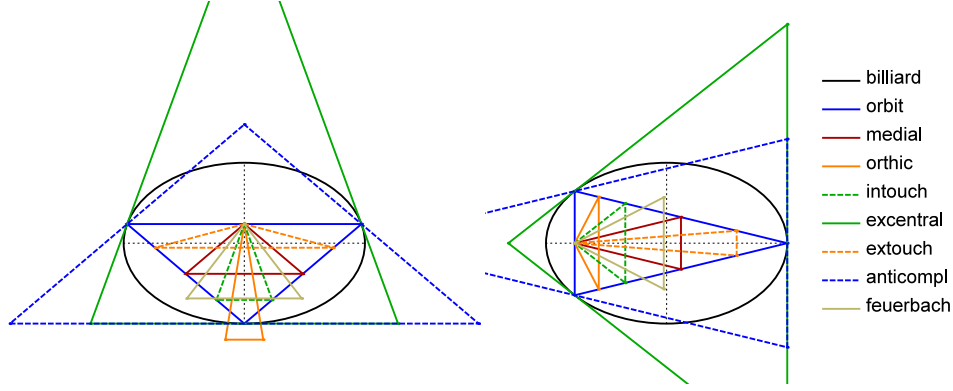


FIGURE 7. The orbit is an isosceles triangle (solid blue) if one of its vertices coincides with either EB vertex. In this situation, any Derived Triangle will contain one vertex on the axis of symmetry of the orbit, Lemma 3. **Video:** [20, pl#08]

Proof. It is similar to that of lemma 2, since any derived triangle of an isosceles orbit has a vertex on the axis of symmetry of the orbit. \square

3.3. Triple Winding of Triangle Center. Let the EB be parametrized by $(a \cos t, b \sin t)$. Let t^* (resp. t^{**}) be the value of t for which the 3-periodic orbit is an isosceles with a horizontal (resp. vertical) axis of symmetry, Figure 8, $t^* > t^{**}$. It can be shown that⁹:

$$\tan t^* = \frac{b\sqrt{2\delta - a^2 + 2b^2}}{a^2}, \quad \tan t^{**} = \frac{\sqrt{2\delta - 2a^2 + b^2}}{\sqrt{3}a}$$

Referring to Figure 8:

Observation 1. *A continuous counterclockwise motion of $P_1(t)$ along the intervals $[-t^*, -t^{**})$, $[-t^{**}, 0)$, $[0, t^{**})$, and $[t^{**}, t^*)$ will each cause X_i to execute a quarter turn along its locus, i.e., with t varying from $-t^*$ to t^* , X_i will execute one complete revolution on its locus¹⁰.*

Observation 2. *A continuous counterclockwise motion of $P_1(t)$ in the $[t^*, \pi - t^*)$ (resp. $[\pi - t^*, \pi + t^*)$, and $[\pi + t^*, 2\pi - t^*)$), visits the same triangles when t sweeps $[-t^*, -t^{**})$ (resp. $[-t^*, t^*)$, and $[t^*, \pi - t^*)$).*

⁹It turns out $\sin t^* = b\gamma$ and $\cos t^{**} = a\gamma$, Joachmishal's constant, Appendix B.4.

¹⁰The direction of this revolution depends on X_i and its not always monotonic. The observation is valid for elliptic or non-elliptic loci alike.

Therefore, a complete turn of $P_1(t)$ around the EB visits the 3-periodic family thrice, and causes X_i to wind thrice on its locus.

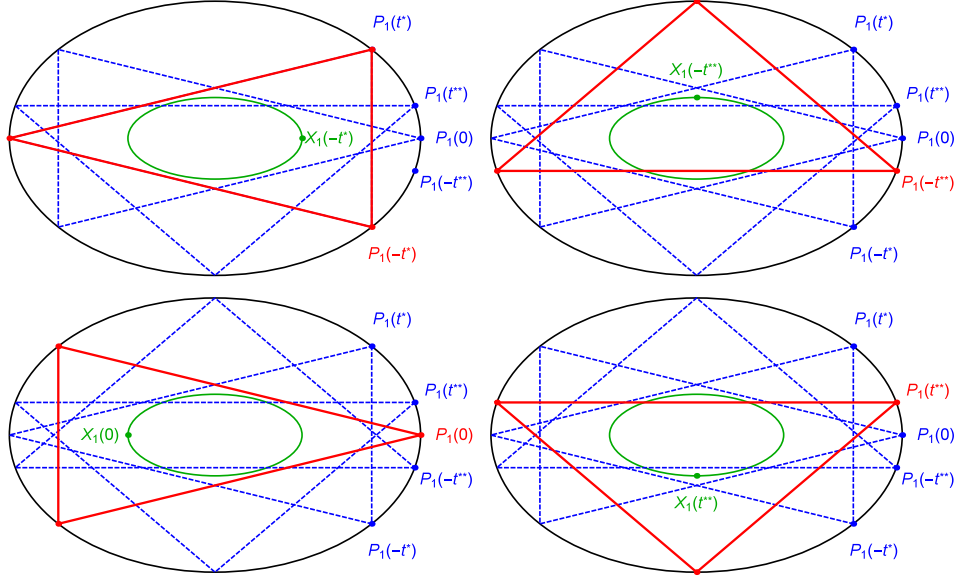


FIGURE 8. Counterclockwise motion of $P_1(t)$, for $t = [-t^*, t^*]$ can be divided in four segments delimited by $t = (-t^*, -t^{**}, 0, t^{**}, t^*)$. Orbit positions for the first four are shown (red polygons) in the top-left, top-right, bot-left, and bot-right pictures. At $P_1(\pm t^*)$ (resp. $P_1(\pm t^{**})$) the orbit is an isosceles triangle with a horizontal (resp. vertical) axis of symmetry. Observations 1,2 assert that a counterclockwise motion of $P_1(t)$ along each of the four intervals causes a Triangle Center X_i to execute a quarter turn along its locus (elliptic or not), and that a complete revolution of $P_1(t)$ around the EB causes X_i to wind thrice on its locus. For illustration, the locus of $X_1(t)$ is shown (green) at each of the four interval endpoints.

4. MAIN RESULT #2: WHEN ARE LOCI ALGEBRAIC?

Theorem 2. *If the Trilinear coordinates of X_i are rational on the sidelengths, then its locus is an implicit algebraic curve.*

Proof. We use the theory of Resultants [13, Chapter IX]. We refer to Lemmas 4 and 5 appearing below.

Assume the Triangle Center Function h (Equation (2)) is a rational function of the sidelengths s_1, s_2, s_3 .

Convert $X_i(u)$ to Cartesians via Equation (3). From Lemma 4, it follows that $(x_i(u), y_i(u))$ are rational on $u, u_1, u_2, s_1, s_2, s_3$. Equivalently, if p, q, r, t are polynomials on said variables, express $x_i(\dots) = p_i(\dots)/q_i$ and $y_i(\dots) = r_i(\dots)/t_i(\dots)$.

Consider the equations $x_i(u) - x = 0$ and $y_i(u) - y = 0$ which are equivalent to the algebraic equations:

$$E_0 = p_i - q_i x = 0, \quad F_0 = r_i - y t_i = 0$$

Let g_1 , g_2 and g_3 be the polynomials in Appendix D. Consider the resultant equations:

$$E_1 = \text{Res}(g_1, E_0, s_1) = 0$$

$$F_1 = \text{Res}(g_1, F_0, s_1) = 0$$

$$E_2 = \text{Res}(g_2, E_1, s_2) = 0$$

$$F_2 = \text{Res}(g_2, F_1, s_2) = 0$$

$$E_3 = \text{Res}(g_3, E_2, s_3) = 0$$

$$F_3 = \text{Res}(g_3, F_2, s_3) = 0$$

From above it follows that $E_3(x, u, u_1, u_2) = 0$ and $F_3(y, u, u_1, u_2) = 0$ are polynomial in these variables. Eliminate the variables u_1 and u_2 by taking the following resultants:

$$E_4(x, u, u_2) = \text{Res}(E_3, u_1^2 + u^2 - 1, u_1) = 0$$

$$F_4(y, u, u_2) = \text{Res}(F_3, u_1^2 + u^2 - 1, u_1) = 0$$

$$E_5(x, u) = \text{Res}(E_4, u_2^2 + \rho u^2 - 1, u_2) = 0$$

$$F_5(y, u) = \text{Res}(F_4, u_2^2 + \rho u^2 - 1, u_2) = 0$$

This yields two polynomial equations $E_5(x, u) = 0$ and $F_5(y, u) = 0$. So $\text{Res}(E_5, F_5, u) = 0$ is the implicit algebraic equation of the locus X_i . This ends the proof. \square

Lemma 4. *Let $P_1 = (au, b\sqrt{1-u^2})$. The coordinates of P_2 and P_3 of the 3-periodic billiard orbit are rational functions in the variables u, u_1, u_2 , where $u_1 = \sqrt{1-u^2}$, $u_2 = \sqrt{1-\rho u^2}$ and $\rho = (a^2 - b^2)^3 / (a(b^2 - \delta))^2$.*

Proof. Follows directly from the parametrization of the billiard orbit, Appendix B.2. In fact, $P_2 = (x_2(u), y_2(u)) = (p_{2x}/q_2, p_{2y}/q_2)$ and $P_3 = (x_3(u), y_3(u)) = (p_{3x}/q_3, p_{3y}/q_3)$, where p_{2x} , p_{2y} , p_{3x} and p_{3y} are algebraic of degree 4 in the variables (u, u_1, u_2) and q_2 , q_3 are algebraic of degree 4 in the variable u . \square

Lemma 5. *Let $P_1 = (au, b\sqrt{1-u^2})$. Let s_1 , s_2 and s_3 the sides of the triangular orbit $P_1 P_2 P_3$. Then $g_1(u, s_1) = 0$, $g_2(s_2, u_2, u) = 0$ and $g_3(s_3, u_2, u) = 0$ for polynomial functions g_i .*

Proof. Using the parametrization of the 3-periodic billiard orbit it follows that $s_1^2 - |P_2 - P_3|^2 = 0$ is a rational equation in the variables u, s_1 . Simplifying, leads to $g_1(s_1, u) = 0$.

Analogously for s_2 and s_3 . In this case, the equations $s_2^2 - |P_1 - P_3|^2 = 0$ and $s_3^2 - |P_1 - P_2|^2 = 0$ have square roots $u_2 = \sqrt{1-\rho u^2}$ and $u_1 = \sqrt{1-u^2}$

and are rational in the variables s_2, u_2, u_1, u and s_3, u_2, u_1, u respectively. It follows that the degrees of g_1 , g_2 , and g_3 are 10. Simplifying, leads to $g_2(s_2, u_2, u_1, u) = 0$ and $g_3(s_3, u_2, u_1, u) = 0$. \square

5. DELIGHTFUL PHENOMENA

Here we describe a variety of phenomena involving the loci of orbit centers and derived triangles. Referring to Equation (1), a, b are the lengths of major and minor semiaxes of the EB.

5.1. Locus of Orthocenter X_4 is similar to rotated EB. Theorem 1 asserts that the locus of the Orthocenter X_4 is an ellipse similar to a rotated copy of the EB. Appendix C.4 shows that when $a/b = a_4^* \simeq 1.51$, the locus is a perpendicular copy of the EB, and for $a/b = a_4 \simeq 1.352$ the locus is tangent to the EB at its top and bottom vertices.

Theorem 3. *If $a/b < a_4$ (resp. $a/b > a_4$) the orbit family will (resp. will not) contain obtuse triangles.*

Proof. If the orbit is acute, X_4 is in its interior, therefore also internal to the EB. If the orbit is a right triangle, X_4 lies on the right-angle vertex and is therefore on the EB. If the orbit is obtuse, X_4 lies on exterior wedge between sides incident on the obtuse vertex (feet of altitudes are exterior). Since the latter is on the EB, X_4 is exterior to the EB. \square

This can be seen in Figure 9.

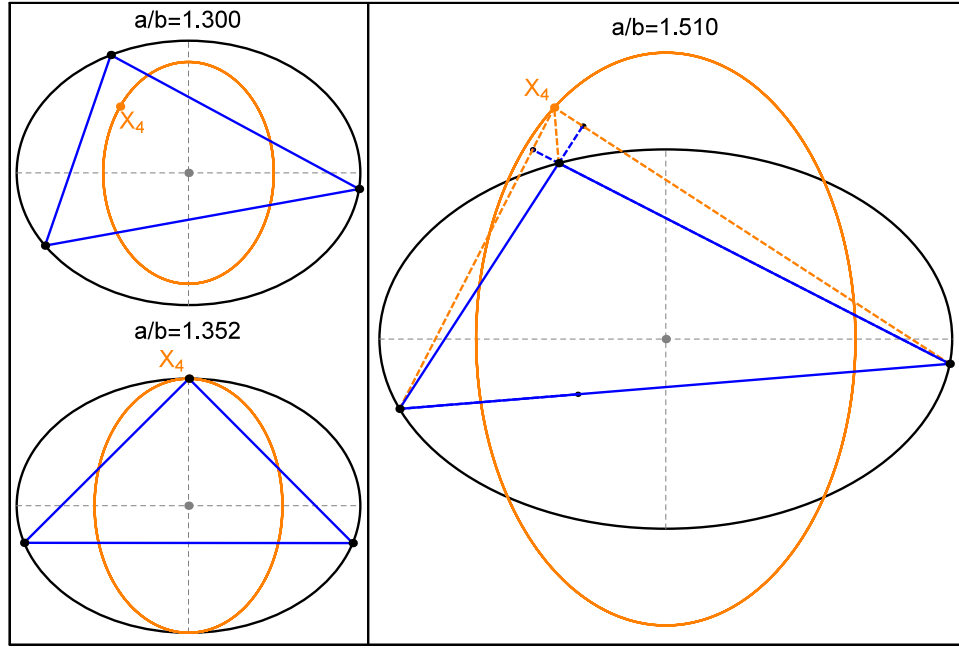


FIGURE 9. Let $a_4 \simeq 1.352$ and H be the elliptic locus of X_4 (orange), similar to a rotated copy of the EB (black). **Top Left:** $a/b < a_4$, H is interior to the EB and all orbits (blue) are acute **Bot Left:** at $a/b = a_4$, H is tangent to the top and bottom vertices of the EB. The orbit shown is a right triangle since one vertex is at the upper EB vertex where X_4 currently is. **Right:** at $a/b > a_4$, the 3-periodic family will contain both acute and obtuse orbits, corresponding to X_4 interior (resp. exterior) to the EB. For any obtuse orbit, X_4 will lie within the wedge between sides incident upon the obtuse angle and exterior to the orbit, i.e., exterior to the EB. For the particular aspect ratio shown ($a/b = 1.51$), H is identical to a 90° -rotated copy of the EB.

5.2. Incenter of Orthic can be a 4-piecewise ellipse. Let T be a triangle, T_h its Orthic¹¹, and I_h be the latter's Incenter. If T is acute, I_h coincides with T 's Orthocenter X_4 . For obtuse T , I_h becomes “pinned” to the vertex subtending the obtuse angle [2, Chapter 1].

Assume $a/b > a_4$. Since the orbit family contains both acute and obtuse triangles, the locus of I_h will switch smoothly between the following regimes:

| orbit | X_4 wrt EB | I_h location |
|----------------|---------------------------|----------------------|
| acute | interior | Orthocenter X_4 |
| right triangle | on it | right-angle vertex |
| obtuse | external (orbit Excenter) | obtuse vertex, on EB |

In turn, this produces a 4-piecewise elliptic locus for I_h , as shown in Figure 10 and [18, pl#11].

¹¹Its vertices are the feet of the altitudes.

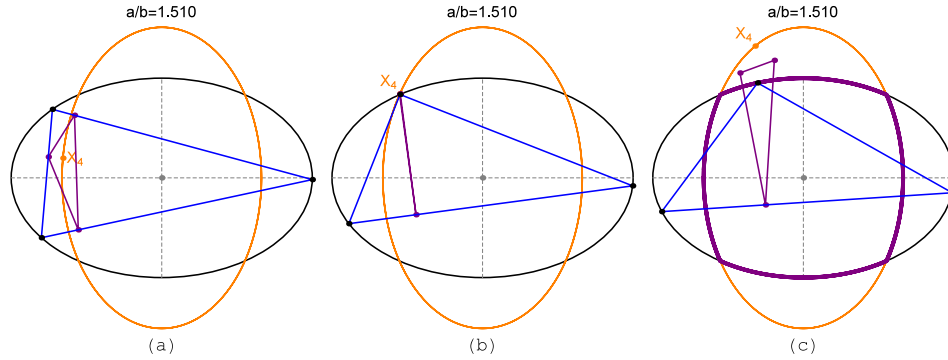


FIGURE 10. An $a/b > a_4$ EB is shown (black). Let T and T_h be the orbit and its Orthic Triangle (blue and purple, respectively). **(a)** T is acute (X_4 is interior to the EB), and $I_h = X_4$. **(b)** X_4 is on the EB and T is a right triangle. T_h degenerates to a segment. **(c)** X_4 is exterior to the EB. Two of T_h 's vertices are outside T . I_h is pinned to T 's obtuse vertex, on the EB. X_4 is an Excenter of the Orbit. The complete locus of I_h comprises therefore 4 elliptic arcs (thick purple). **Video:** [18, pl#11]

Observation 3. *If $a/b > a_4$ the locus of the Incenter of the orbit's Orthic Triangle comprises four arcs of ellipses, i.e., it contains four kinks.*

5.3. Extouchpoints sweep the caustic.

Theorem 4. *The Extouchpoints sweeps the Caustic.*

The Inconic centered on the Mittenpunkt X_9 and passes through the Extouchpoints is known as the *Mandart Inellipse* [28]. By definition, an Inconic is internally tangent to the sides, so it must be the Caustic. Besides always being on the Caustic, the locus of the Extouchpoints cover it, Lemma 3. This can be seen in Figure 1 (right), and on a video [20, pl#07].

5.4. Anticomplementary Intouchpoints are on the EB. Consider a 3-periodic's Anticomplementary Triangle (ACT) [28] and its Intouchpoints i'_1, i'_2, i'_3 , Figure 11. Remarkably [18, pl #12]:

Theorem 5. *The locus of the Anticomplementary Triangle's Intouchpoints is the EB.*

Proof. Consider an elementary triangle with vertices $Q_1 = (0, 0)$, $Q_2 = (1, 0)$ and $Q_3 = (u, v)$. Its sides are $s_1 = |Q_3 - Q_2|$, $s_2 = |Q_3 - Q_1|$, and $s_3 = 1$.

Let E be its *Circumbilliard*, i.e., the Circumellipse for which $Q_1Q_2Q_3$ is a 3-periodic EB trajectory. The following implicit equation for E was derived [6]:

$$E(x, y) = v^2 x^2 + (u^2 + (s_1 + s_2 - 1)u - s_2)y^2 + v(1 - s_1 - s_2 - 2u)xy + v(s_2 + u)y - v^2 x = 0$$

The vertices of the ACT are can be derived as $Q'_1 = (u - 1, v)$, $Q'_2 = (u + 1, v)$, and $Q'_3 = (1 - u, -v)$., and its Incenter¹² is:

$$X'_1 = \left[s_1 - s_2 + u, \frac{s_2(s_1 - 1) + (1 - s_1 + s_2)u - u^2}{v} \right].$$

The ACT Intouchpoints are the feet of perpendiculars dropped from X'_1 onto each side of the ACT, and can be derived as:

$$\begin{aligned} i'_1 &= \left[\frac{s_1(u - 1)u + s_2}{s_2}, \frac{v(s_1 - 1)}{s_2} \right] \\ i'_2 &= \left[\frac{(u - 1)(s_2 - 1)}{s_2}, \frac{(s_2 - 1)v}{s_2} \right] \\ i'_3 &= [s_1 - s_2 + u, v]. \end{aligned}$$

Direct calculations shows that $E(i'_1) = E(i'_2) = E(i'_3) = 0$.

Besides always being on the EB, the locus of the Intouchpoints cover it. Let $P_1(t)P_2(t)P_3(t)$ be a 3-periodic and $P'_1(t)P'_2(t)P'_3(t)$ its ACT. For all t the Intouchpoint $i'_1(t)$ is located on the side $P'_2(t)P'_3(t)$ of the ACT and on the elliptic arc $\text{arc}(P_1(t)P_3(t))$, Figure 11. Therefore, when $P_1(t)$ completes a circuit on the EB, $i'_1(t)$ will have to complete a similar tour. Analogously for $i'_2(t)$ and $i'_3(t)$. \square

¹²This is the Nagel Point X_8 of the original triangle.

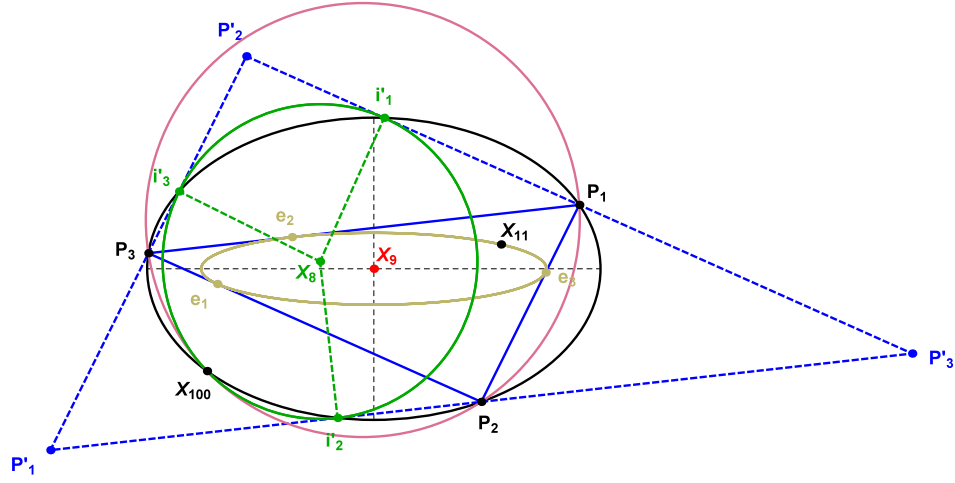


FIGURE 11. A 3-periodic orbit $P_1P_2P_3$ is shown (blue). Shown also is the Mittenpunkt X_9 , at the EB center. The orbit's Anticomplementary Triangle (ACT) $P'_1P'_2P'_3$ (dashed blue) has sides parallel to the orbit. The latter's Intouchpoints i'_1 , i'_2 , and i'_3 are the feet of perpendiculars dropped from the ACT's Incenter (X_8) to each side (dashed green). The ACT's Incircle (green) and 9-point circle (the orbit's Circumcircle, pink) meet at X_{100} , the ACT's Feuerbach Point. Its locus is also the EB. The Caustic is shown brown. On it there lie X_{11} and the three Extouchpoints e_1 , e_2 , e_3 . **Video:** [18, pl#12]

Furthermore, if $P_1(t)$ moves monotonically in one direction, the ACT intouch points will move non-monotonically with respect to $P_1(t)$, Figure 12.

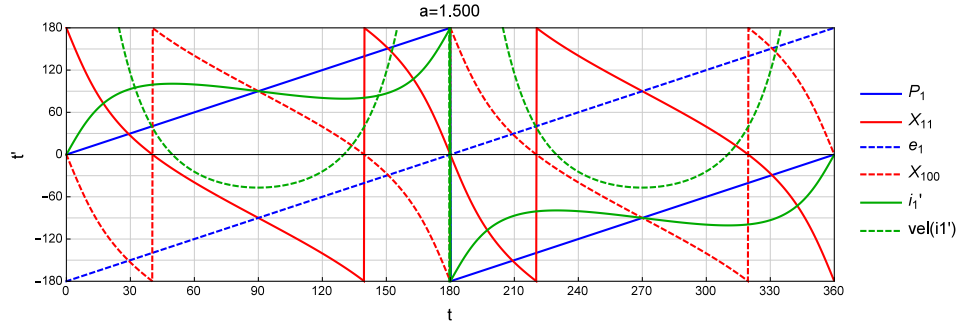


FIGURE 12. Let $P_1(t) = (a \cos(t), b \sin(t))$ slide counterclockwise along the EB. The graph shows the angular location t' of various points on their elliptic loci vs t of P_1 . Namely, (i) X_{11} moves monotonically in the opposite direction of P_1 . (ii) Extouchpoint e_1 moves along the Caustic in the same direction and with the same angular speed as P_1 . (iii) X_{100} moves along the EB monotonically opposite to P_1 . (iv) the Anticomplementary's Intouchpoint i'_1 moves along the EB in both forwards and retrograde fashion, as attested by (v) the sign of its angular velocity (dashed green). Its lowest velocity is achieved at $t = \pi/2$.

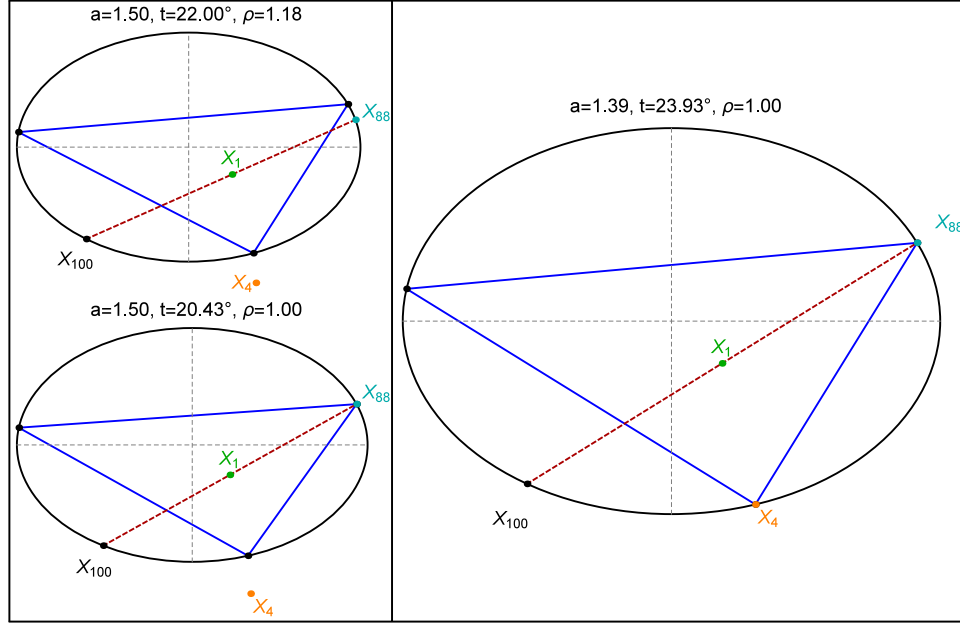


FIGURE 13. X_{88} is always on the EB and collinear with X_1 and X_{100} [12]. Let ρ (shown above each picture) be the ratio $|X_1 - X_{100}|/|X_1 - X_{88}|$. **(a)** The particular orbit shown is obtuse (X_4 is exterior), and $\rho > 1$, i.e., X_1 is closer to X_{88} . **(b)** When X_{88} coincides with a vertex, if sidelengths are ordered as $s_1 \leq s_2 \leq s_3$, then $s_2 = (s_1 + s_3)/2$, and X_1 becomes the midpoint of $X_{88}X_{100}$, i.e., $\rho = 1$. **(c)** If $a/b \simeq 1.39$, when X_{88} is on a vertex, the orbit is a 3 : 4 : 5 triangle (X_4 lies on an alternate vertex). **Video:** [20, pl#13]

5.5. X_{88} sweeps Billiard and can be retrograde. Let P_1 slide counter-clockwise along the EB. Let $a_{88} = (\sqrt{2\sqrt{2} + 6})/2 \simeq 1.485$. It can be shown that if $a/b < a_{88}$, then X_{88} will move monotonically clockwise along the EB. If a/b is greater than this threshold, then the motion of X_{88} will contain four monotonic phases, with its velocity changing sign twice before and after it crosses either horizontal vertex of the EB. This is shown on [20, pl#13].

Let the orbit have sides $s_1 \leq s_2 \leq s_3$. That X_{88} and X_{100} lie on the EB was shown above. For any triangle, X_{88} is collinear with X_1 and X_{100} [12]. The following facts can be shown:

- X_{88} coincides with a vertex orbit if and only if $s_2 = (s_1 + s_3)/2$. In this case, X_1 is the midpoint between X_{100} and X_{88} [9], Figure 13a.
- The only right-triangle orbit for which X_{88} coincides with a vertex requires that $s_1 : s_2 : s_3 = 3 : 4 : 5$.
- The only EB which can contain a 3 : 4 : 5 orbit has an aspect ratio $a/b = (7 + \sqrt{5})\sqrt{11}/22 \simeq 1.3924$, Figure 13b.

The reader is challenged to find an expression for parameter t in $P_1(t)$ where the motion of X_{88} changes direction.

5.6. Locus of Symmedian Point X_6 is a quartic. The Symmedian Point X_6 is the intersection of the Symmedian lines [28]. Interestingly, it is the only Triangular Center out of Kimberling's first 12 whose locus is non-elliptic. For an $a/b = 1.5$, the average distance with respect to a best-fit ellipse is of the order of 10^{-4} , i.e., imperceptible to the naked eye. Figure 14 shows such a scenario where the deviation is exaggerated a million-fold. In fact:

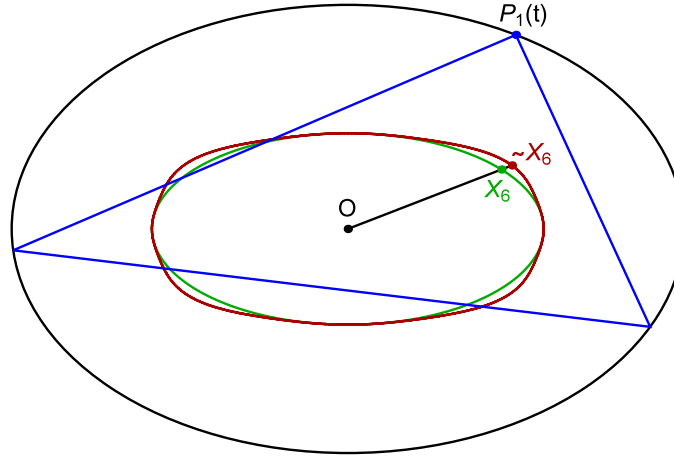


FIGURE 14. The convex, quartic, locus of the Symmedian Point X_6 (green), is indistinguishable to the naked eye from an ellipse at the EB aspect ratio shown ($a/b = 1.5$). The red path shows the locus with the deviation from a best-fit ellipse exaggerated two million-fold.

Observation 4. *The locus of the Symmedian Point X_6 of the 3-periodic family is a convex quartic.*

Observation 5. *An ellipse with axes a_6, b_6 can be found which is internally tangent to the locus of X_6 at its four vertices.*

Details can be found in Appendix E.

5.7. X_{59} is at least sextic with 4 self-intersections. Experimentally, X_{59} is a continuous curve internally tangent to the EB at its four vertices, and with four self-intersections, Figure 15, and as an animation [20, pl#14]. It intersects a line parallel to and infinitesimally away from either axis on six points, so its degree must be at least 6. The following are unsolved (reader feedback is welcome).

- What is the degree of its implicit?
- What is t in $P_1(t) = (a \cos(t), b \sin(t))$ such that X_{59} is on one of the four self-intersections? For example, at $a/b = 1.3$ (resp. 1.5), $t \simeq 32.52^\circ$ (resp. 29.09° , Figure 15 (left-bottom)).

- What is a/b such that if X_{59} is on one of the lower self-intersection on the y -axis, the orbit is a right triangle? Numerically, this occurs when $a/b \simeq 1.58$ and $t \simeq 27.92^\circ$, Figure 15 (right).

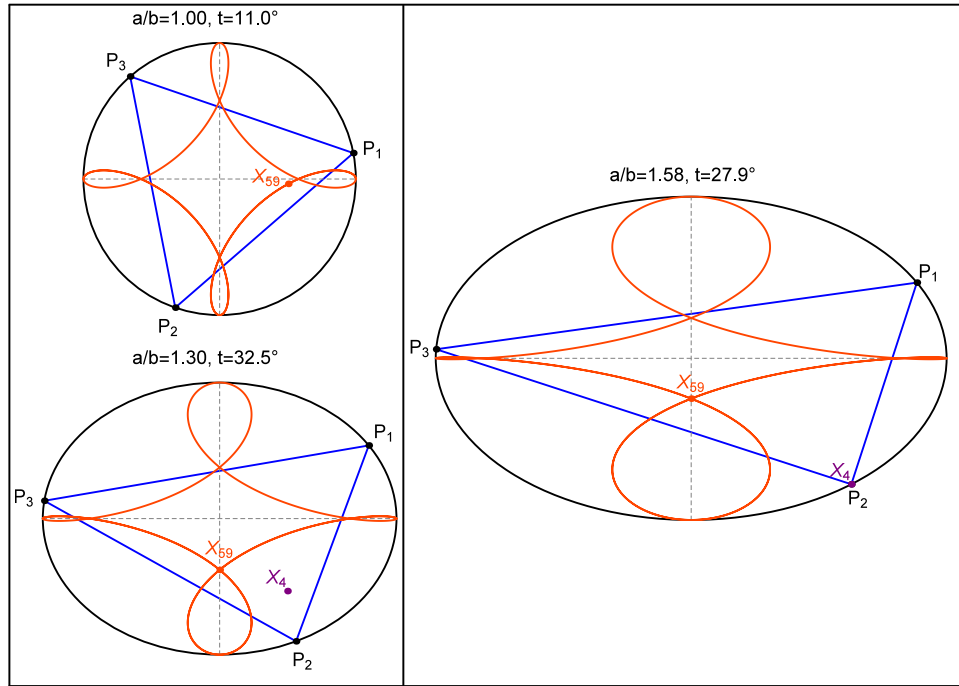


FIGURE 15. The locus of X_{59} is a continuous curve with four self-intersections, and at least a sextic. It is tangent to the EB at its four vertices. **Top Left:** circular EB, X_{59} is symmetric about either axis. **Bottom Left:** $a/b = 1.3$, at $t \simeq 32.5^\circ$ X_{59} is at the lower self-intersection and the orbit is acute (X_4 is interior). **Right:** at $a/b \simeq 1.58$ the following feat is possible: X_{59} is at the lower self-intersection and the orbit is a right-triangle (X_4 is on P_2). This occurs at $t \simeq 27.9^\circ$. **Video:** [20, pl#14]

5.8. The locus of X_{26} can be non-compact. X_{26} is the Circumcenter of the Tangential Triangle [28]. Its sides are tangent to the Circumcircle at the vertices. Therefore X_{26} of a right-triangle is at infinity. When $a/b \geq a_4$, the 3-periodic family will contain 2 (or 4) right triangles, therefore the locus of X_{26} will only be compact when $a/b < a_4$, Figure 16.

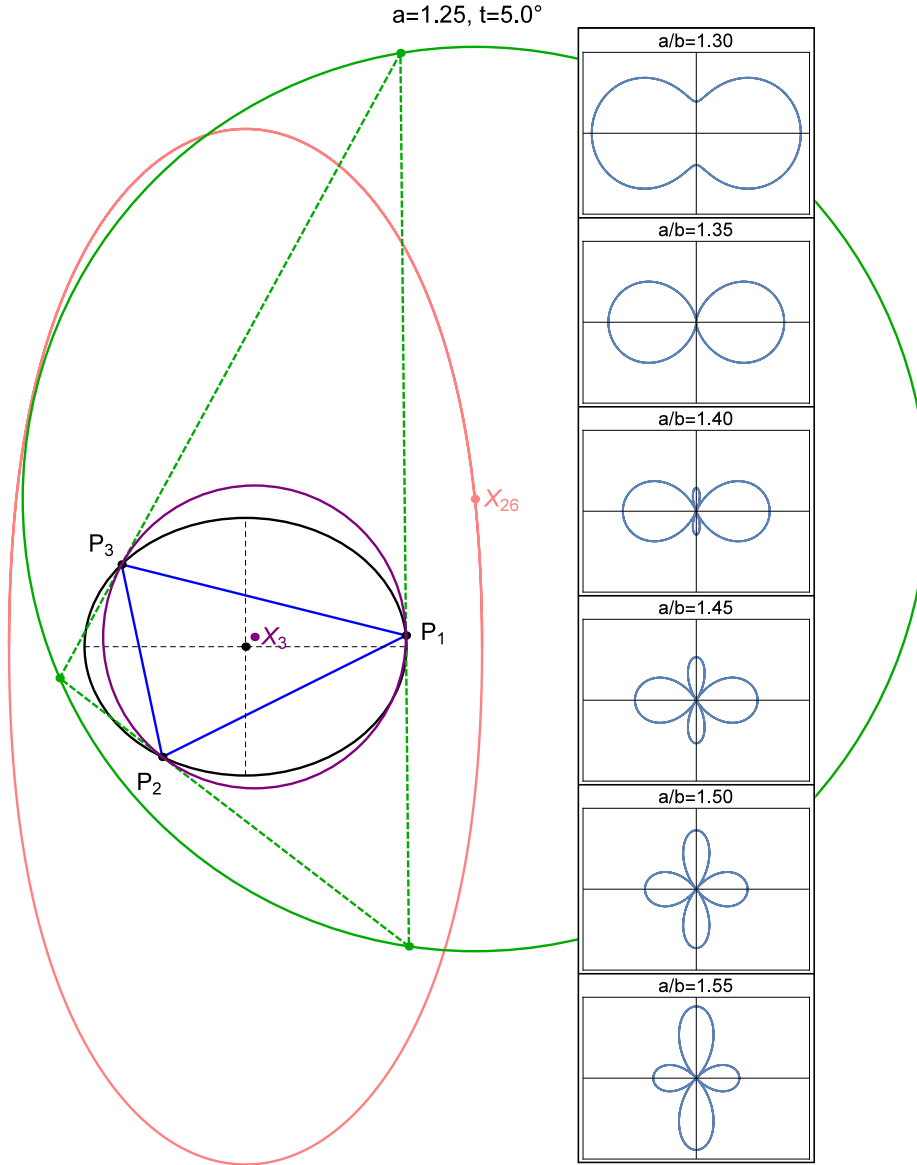


FIGURE 16. The locus of X_{26} for a 3-periodic orbit (blue) in an $a/b = 1.25$ EB (black). Also shown is the orbit's Circumcircle (purple) and its Tangential Triangle [28] (dashed green). X_{26} is the center of the latter's Circumcircle (solid green). Its locus is non-elliptic. In fact, when $a/b \geq a_4$, the orbit family will contain right-triangles (X_4 crosses the EB). At these events, X_{26} goes to infinity. The right inset shows an inversion of X_{26} with respect to the EB center for various values of a/b . When $a/b > a_4$, the inversion goes through the origin, i.e., X_{26} is at infinity.

5.9. The locus of X_{40} makes the EB golden. The *Bevan Point* X_{40} is the Excentral Triangle's Circumcenter [12]. Its locus is an ellipse similar to a rotated copy of the Billiard with axes (Appendix C.15):

$$a_{40} = (a^2 - b^2)/a, \quad b_{40} = (a^2 - b^2)/b.$$

If one imposes $b_{40} = a$, then $a/b = (1 + \sqrt{5})/2$, i.e., when the aspect ratio is the Golden Ratio, the locus of X_{40} is identical to a 90° -rotated copy of the EB, Figure 17. A video of this curious phenomenon is available [20, pl#15].

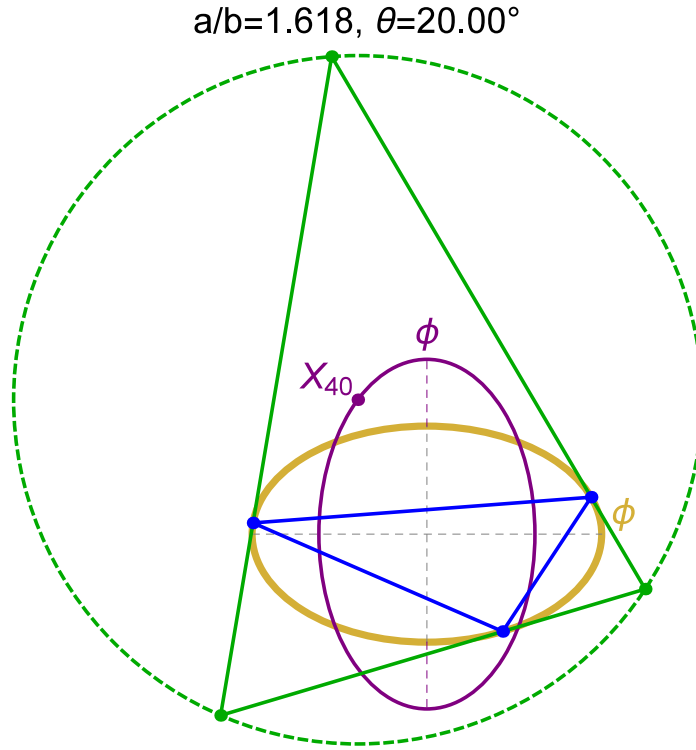


FIGURE 17. An $a/b = \phi \simeq 1.618$ EB is shown (gold). The Bevan Point X_{40} is the Circumcenter of the Excentral Triangle (solid green). A 3-periodic orbit is shown (blue). At this aspect ratio, the locus of X_{40} (purple) is a 90° rotated copy of the EB. **Video:** [20, pl#15].

5.10. Elliptic Loci are degenerate triple-winding curves. Though we have been describing certain loci as ellipses, algebraically, their locus satisfies the equation of an ellipse raised to third power, i.e., every point on it has multiplicity 3.

Parametrically, they are the limit case of analytic curves that turn thrice about the center of the EB for every turn of $P_1(t)$. As an example, Figure 18 shows the locus of a point midway between the Incenter X_1 and one of the Intouchpoints. If said intermediate point is close to (resp. far from) X_1 , the

locus is a tightly-wound 3-loop curve (resp. a triple-winding curve with two internal lobes). In the former (resp. latter) case, the locus is the X_1 ellipse (resp. the Intouch locus, known to be a two-lobe curve [21]).

The same phenomenon can be observed for loci of convex combinations of the following pairs: (i) Barycenter X_2 and a side midpoint, (ii) Circumcenter X_3 and a foot of a side midpoint, (iii) Orthocenter X_4 and altitude foot, as shown in [20, pl#16,17].

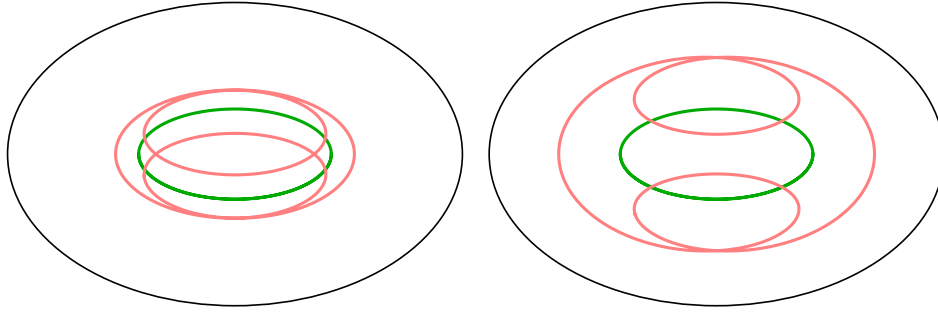


FIGURE 18. The locus of X_1 is the limit case of a curve with two internal lobes. Drive by a single clockwise motion of $P_1(t)$, X_1 loop thrice over its elliptic locus (solid green). **Left:** The locus (pink) of a point 30% of the way between X_1 and an Intouchpoint (not shown). Notice the two internal lobes. **Right:** the same locus when the intermediate point is 80% of the way from X_1 to an Intouchpoint. **Video:** [20, pl#16,17]

5.11. Summary of Phenomena. Tables 2 and 3 respectively summarize this Section's various loci phenomena, and notable a/b thresholds.

| Point | Type of Locus | Comments |
|--------------|--|---|
| X_1 | Ellipse | Limit of curve with two-internal loops |
| X_4 | Ellipse | Inside EB when $a < a_4$ |
| X_6 | Convex Quartic | Externally-Tangent to ellipse (a_6, b_6) , Appendix E |
| X_{26} | Non-Elliptic | When $a/b \geq a_4$, goes to ∞ when orbit is right triangle |
| X_{59} | At Least Sextic | 4 Self-Intersections |
| X_{88} | Ellipse | EB, retrograde when $a/b > a_{88}$ |
| Orthic X_1 | If $a < a_4$ is X_4 locus, else 4-piecewise ellipse | 4-piecewise: 2 arcs from X_4 locus, and 2 arcs from EB |
| Extouch | Ellipse | Caustic |
| ACT Intouch | Ellipse | EB |

TABLE 2. Loci phenomena for various Triangle Centers mentioned in Section 5.

| symbol | a/b | Significance |
|----------------|-------|--|
| a_4 | 1.352 | locus of X_4 is tangent to EB. above it, some orbits are obtuse |
| a_{88}^\perp | 1.392 | with X_{88} on a vertex, sidelengths are 3 : 4 : 5 |
| a_{88} | 1.486 | above it, motion of X_{88} is non-monotonic |
| a_4^* | 1.510 | X_4 locus identical to rotated EB |
| a_{59}^\perp | 1.580 | when X_{59} is at self-intersection, orbit is right triangle |
| ϕ | 1.618 | X_{40} locus identical to rotated EB |

TABLE 3. A few thresholds for a/b and their effects on loci phenomena.

6. CONCLUSION

A gallery of loci generated by X_1 to X_{100} (as well as vertices of derived triangles) is provided in [19]. The reader is invited to interact with loci for various Triangle Centers using our online applet [17]. Videos mentioned herein are on a public playlist [20], with links provided on Table 4.

| PL# | Title | Section |
|-----|---|---------|
| 01 | Locus of X_1 is an Ellipse | 1 |
| 02 | Locus of Intouchpoints is non-elliptic | 1, 2 |
| 03 | X_9 stationary at EB center | 1 |
| 04 | Stationary Excentral Cosine Circle | 1 |
| 05 | Loci for $X_1 \dots X_5$ are ellipses | 2 |
| 06 | Elliptic locus of Excenters similar to rotated X_1 | 2 |
| 07 | Loci of X_{11} , X_{100} and Extouchpoints are the EB | 2, 5.3 |
| 08 | Family of Derived Triangles | 3 |
| 09 | Loci of Vertices of Derived Triangles | 2,3 |
| 10 | Peter Moses' 29 Billiard Points | 3 |
| 11 | Locus of Orthic Incenter is 4-piece ellipse | 5.1 |
| 12 | Intouchpoints of Anticompl. Triangle on the EB | 5.4 |
| 13 | Locus of X_{88} is on the EB and can be retrograde | 5.5 |
| 14 | Locus of X_{59} with 4 self-intersections | 5.7 |
| 15 | Locus of X_{40} and the Golden Billiard | 5.9 |
| 16 | Locus of Convex Comb.: X_1 -Intouch and X_2 -Midpoint | 5.10 |
| 17 | Locus of Convex Comb.: X_3 -Midpoint and X_4 -Altfoot | 5.10 |

TABLE 4. Videos mentioned in the paper. Column “PL#” indicates the entry within the playlist [20].

The following are interesting questions we would invite the reader to contribute.

- Is there a condition for the Trilinears of a Triangle Center so that its locus is an ellipse? Table 5 for a few examples showing no apparent pattern.
- Can the degree of the locus of a Triangle Center or Derived Triangle vertex be predicted without long calculations?
- Can a Triangle Center be found such that its locus can intersect a straight line more than 6 times?
- Certain Triangles Centers have non-convex loci (e.g., X_{67} at $a/b = 1.5$ [19]). What determines non-convexity?
- What determines the number of self-intersections of a given locus?
- In the spirit of [22, 4], how would one determine via complex analytic geometry, that X_6 is a quartic?

| center | name | $h(s_1, s_2, s_3)$ | $h_\theta(\theta_1, \theta_2, \theta_3)$ |
|---------------------|---|--|---|
| X_1 | Incenter | 1 | |
| X_2 | Centroid | $1/s_1$ | $\cos \theta_1 + \cos(\theta_2 - \theta_3)$ |
| X_3 | Circumcenter | $s_1(s_2^2 + s_3^2 - s_1^2)$ | $\cos \theta_1$ |
| X_4 | Orthocenter | $1/[s_1(s_2^2 + s_3^2 - s_1^2)]$ | $\sec \theta_1$ |
| X_5 | 9-Point Center | $s_2 s_3 [s_1^2(s_2^2 + s_3^2) - (s_2^2 - s_3^2)^2]$ | $\cos(\theta_2 - \theta_3)$ |
| \mathbf{X}_6^* | Symmedian Point | s_1 | $\sin \theta_1$ |
| X_9 | Mittenpunkt | $s_2 + s_3 - s_1$ | $\cot(\theta_1/2)$ |
| X_{11} | Feuerbach Point | $s_2 s_3 (s_2 + s_3 - s_1)(s_2 - s_3)^2$ | $1 - \cos(\theta_2 - \theta_3)$ |
| \mathbf{X}_{59}^* | Isog. Conj. of X_{11} | $1/[s_2 s_3 (s_2 + s_3 - s_1)(s_2 - s_3)^2]$ | $1/[1 - \cos(\theta_2 - \theta_3)]$ |
| \mathbf{X}_{19}^* | Clawson Point | $1/(s_2^2 + s_3^2 - s_1^2)$ | $\tan(\theta_1)$ |
| X_{88} | Isog. Conjug. of X_{44} | $1/(s_2 + s_3 - 2s_1)$ | |
| X_{100} | Anticomplement of X_{11} | $1/(s_2 - s_3)$ | |

TABLE 5. Triangle Center function h for a few Triangle Centers, both in terms of sidelengths $h(s_1, s_2, s_3)$ and angles $h_\theta(\theta_1, \theta_2, \theta_3)$. X_6 , X_{19} , and X_{59} are starred/boldfaced as their locus is non-elliptic (all others are except X_9 which is a point). We haven't yet detected an algebraic pattern which differentiates both groups.

ACKNOWLEDGMENTS

We would like to thank Sergei Tabachnikov, Richard Schwartz, Arseniy Akopyan, Olga Romaskevich, Corentin Fierobe, Ethan Cotterill, and Mark Helman for generously helping us during this research.

The second author is fellow of CNPq and coordinator of Project PRONEX/CNPq/ FAPEG 2017 10 26 7000 508.

REFERENCES

- [1] Akopyan, A., Schwartz, R., Tabachnikov, S.: Billiards in ellipses revisited (2020). URL <https://arxiv.org/pdf/2001.02934.pdf>
- [2] Coxeter, H.S.M., Greitzer, S.L.: Geometry Revisited, *New Mathematical Library*, vol. 19. Random House, Inc., New York (1967)
- [3] Dragović, V., Radnović, M.: Poncelet Porisms and Beyond: Integrable Billiards, Hyperelliptic Jacobians and Pencils of Quadrics. *Frontiers in Mathematics*. Springer, Basel (2011). URL <https://books.google.com.br/books?id=QcOmDAEACAAJ>
- [4] Fierobe, C.: On the circumcenters of triangular orbits in elliptic billiard (2018). URL <https://arxiv.org/pdf/1807.11903.pdf>. Submitted
- [5] Fitzgibbon, A., Pilu, M., Fisher, R.: Direct least square fitting of ellipses. *Pattern Analysis and Machine Intelligence* **21**(5) (1999)
- [6] Garcia, R.: Elliptic billiards and ellipses associated to the 3-periodic orbits. *American Mathematical Monthly* **126**(06), 491–504 (2019). URL <https://doi.org/10.1080/00029890.2019.1593087>
- [7] Griffiths, P., Harris, J.: On Cayley's explicit solution to Poncelet's porism. *Enseign. Math.* (2) **24**(1-2), 31–40 (1978)
- [8] Grozdev, S., Dekov, D.: The computer program "IJDiscoverer" as a tool of mathematical investigation. *International Journal of Computer Discovered Mathematics (IJCDM)* (2014). URL <http://www.ddekov.eu/j/2014/JCGM201405.pdf>
- [9] Helman, M.: Proofs related to locus of X_{88} . Private Communication (January, 2020)

- [10] Kaloshin, V., Sorrentino, A.: On the integrability of Birkhoff billiards. *Phil. Trans. R. Soc. A* (376) (2018). DOI <https://doi.org/10.1098/rsta.2017.0419>
- [11] Kimberling, C.: Triangle centers as functions. *Rocky Mountain J. Math.* **23**(4), 1269–1286 (1993). DOI 10.1216/rmjm/1181072493. URL <https://doi.org/10.1216/rmjm/1181072493>
- [12] Kimberling, C.: Encyclopedia of triangle centers (2019). URL <https://faculty.evansville.edu/ck6/encyclopedia/ETC.html>
- [13] Lang, S.: Algebra, *Graduate Texts in Mathematics*, vol. 211, third edn. Springer-Verlag, New York (2002). DOI 10.1007/978-1-4613-0041-0. URL <https://doi.org/10.1007/978-1-4613-0041-0>
- [14] Levi, M., Tabachnikov, S.: The Poncelet grid and billiards in ellipses. *The American Mathematical Monthly* **114**(10), 895–908 (2007). DOI 10.1080/00029890.2007.11920482. URL <https://doi.org/10.1080/00029890.2007.11920482>
- [15] Moore, R., Kearfott, R.B., Cloud, M.J.: Introduction to Interval Analysis. SIAM (2009)
- [16] Pugh, C.C.: Real mathematical analysis, second edn. Undergraduate Texts in Mathematics. Springer, Cham (2015). DOI 10.1007/978-3-319-17771-7. URL <https://doi.org/10.1007/978-3-319-17771-7>
- [17] Reznik, D.: Applet showing the locus of several triangular centers (2019). URL <https://editor.p5js.org/dreznik/full/i1Lin7lt7>
- [18] Reznik, D.: New properties of polygonal orbits in elliptic billiards: Main videos (2019). URL <https://bit.ly/2k5GXbB>
- [19] Reznik, D.: Triangular orbits in elliptic billiards: Loci of points $X(1)$ $X(100)$ (2019). URL https://dan-reznik.github.io/Elliptical-Billiards-Triangular-Orbits/loci_6tri.html
- [20] Reznik, D.: Playlist for “Loci of Triangular Orbits in an Elliptic Billiard” (2020). URL <https://bit.ly/3072LV3>
- [21] Reznik, D., Garcia, R., Koiller, J.: Can the elliptic billiard still surprise us? *Mathematical Intelligencer* (2019). DOI 10.1007/s00283-019-09951-2. URL <https://arxiv.org/pdf/1911.01515.pdf>
- [22] Romaskevich, O.: On the incenters of triangular orbits on elliptic billiards. *Enseign. Math.* **60**(3-4), 247–255 (2014). DOI 10.4171/LEM/60-3/4-2. URL <https://arxiv.org/pdf/1304.7588.pdf>
- [23] Rozikov, U.A.: An Introduction To Mathematical Billiards. World Scientific Publishing Company (2018)
- [24] Schwartz, R., Tabachnikov, S.: Centers of mass of Poncelet polygons, 200 years after. *Math. Intelligencer* **38**(2), 29–34 (2016). DOI 10.1007/s00283-016-9622-9. URL <http://www.math.psu.edu/tabachni/prints/Poncelet5.pdf>
- [25] Snyder, J.M.: Interval analysis for computer graphics. *Computer Graphics* **26**(2), 121–129 (1992)
- [26] Tabachnikov, S.: Geometry and Billiards, *Student Mathematical Library*, vol. 30. American Mathematical Society, Providence, RI (2005). DOI 10.1090/stml/030. URL <http://www.personal.psu.edu/sot2/books/billiardsgeometry.pdf>. Mathematics Advanced Study Semesters, University Park, PA
- [27] Tabachnikov, S.: Projective configuration theorems: old wine into new wineskins. In: S. Dani, A. Papadopoulos (eds.) *Geometry in History*, pp. 401–434. Springer Verlag (2019). URL <https://arxiv.org/pdf/1607.04758.pdf>
- [28] Weisstein, E.: Mathworld (2019). URL <http://mathworld.wolfram.com>

APPENDIX A. TRIANGLE CENTERS

Any point on the plane of a triangle $T = P_1P_2P_3$ can be defined by specifying a triple of *Trilinear Coordinates* $x : y : z$ which are proportional

to the signed distances from P to each side, which makes them invariant under similarity transformations (rigid+dilation).

A *Triangle Center* (with respect to a triangle $T = P_1P_2P_3$) is defined by Trilinear Coordinates obtained by thrice applying a *Triangle Center Function* h to the sidelengths as follows:

$$(2) \quad x : y : z \iff h(s_1, s_2, s_3) : h(s_2, s_3, s_1) : h(s_3, s_1, s_2)$$

h must (i) be *bi-symmetric*, i.e., $h(s_1, s_2, s_3) = h(s_1, s_3, s_2)$, and (ii) homogeneous, $h(ts_1, ts_2, ts_3) = t^n h(s_1, s_2, s_3)$ for some n [11].

A list of Trilinears for a few Triangle Centers is provided on Table 5. Trilinears for 40k+ Triangle centers are available in [12].

The vertices of a *Derived Triangle* are the rows (taken as Trilinears) of a 3x3 *Trilinear Matrix*, whose entries depend on three Triangle Center functions h_1, h_2, h_3 applied as follows:

$$\begin{bmatrix} h_1(s_1, s_2, s_3) & h_2(s_1, s_2, s_3) & h_3(s_1, s_2, s_3) \\ h_3(s_2, s_3, s_1) & h_1(s_2, s_3, s_1) & h_2(s_2, s_3, s_1) \\ h_2(s_3, s_1, s_2) & h_3(s_3, s_1, s_2) & h_1(s_3, s_1, s_2) \end{bmatrix}$$

Trilinears can be converted to Cartesians using [28]:

$$(3) \quad X_i|_{\text{cartesian}} = \frac{s_1xP_1 + s_2yP_2 + s_3zP_3}{D}$$

Where and $D = s_1x + s_2y + s_3z$.

APPENDIX B. BILLIARD OBJECTS: EXPLICIT EXPRESSIONS

Let the boundary of the Billiard satisfy Equation (1). Assume, without loss of generality, that $a \geq b$.

B.1. Exit Angle Required for 3-Periodicity. Consider a starting point $P_1 = (x_1, y_1)$ on a Billiard with semi-axes a, b . The cosine of the exit angle α (measured with respect to the normal at P_1 ¹³) required for the trajectory to close after 3 bounces is given by [6]:

$$(4) \quad \cos \alpha = \frac{a^2b\sqrt{2\delta - a^2 - b^2}}{c^2\sqrt{a^4 - c^2x_1^2}}, \quad c^2 = a^2 - b^2, \quad \delta = \sqrt{a^4 - a^2b^2 + b^4}.$$

¹³i.e., $\alpha = \theta_1/2$.

B.2. Orbit Vertices. Given a starting vertex P_1 and an exit angle α (as above), the orbit $P_1P_2P_3$ will be such that [6]:

vertex P_2 will be given by $(p_{2x}, p_{2y})/q_2$, with

$$\begin{aligned} p_{2x} &= -b^4 \left((a^2 + b^2) \cos^2 \alpha - a^2 \right) x_1^3 - 2a^4 b^2 \cos \alpha \sin \alpha x_1^2 y_1 \\ &\quad + a^4 \left((a^2 - 3b^2) \cos^2 \alpha + b^2 \right) x_1 y_1^2 - 2a^6 \cos \alpha \sin \alpha y_1^3, \\ p_{2y} &= 2b^6 \cos \alpha \sin \alpha x_1^3 + b^4 \left((b^2 - 3a^2) \cos^2 \alpha + a^2 \right) x_1^2 y_1 \\ &\quad + 2a^2 b^4 \cos \alpha \sin \alpha x_1 y_1^2 - a^4 \left((a^2 + b^2) \cos^2 \alpha - b^2 \right) y_1^3 \\ q_2 &= b^4 \left(a^2 - c^2 \cos^2 \alpha \right) x_1^2 + a^4 \left(b^2 + c^2 \cos^2 \alpha \right) y_1^2 \\ &\quad - 2a^2 b^2 c^2 \cos \alpha \sin \alpha x_1 y_1. \end{aligned}$$

and vertex P_3 will be given by $(p_{3x}, p_{3y})/q_3$, with:

$$\begin{aligned} p_{3x} &= b^4 \left(a^2 - (b^2 + a^2) \right) \cos^2 \alpha x_1^3 + 2a^4 b^2 \cos \alpha \sin \alpha x_1^2 y_1 \\ &\quad + a^4 \left(\cos^2 \alpha (a^2 - 3b^2) + b^2 \right) x_1 y_1^2 + 2a^6 \cos \alpha \sin \alpha y_1^3 \\ p_{3y} &= -2b^6 \cos \alpha \sin \alpha x_1^3 + b^4 \left(a^2 + (b^2 - 3a^2) \cos^2 \alpha \right) x_1^2 y_1 \\ &\quad - 2a^2 b^4 \cos \alpha \sin \alpha x_1 y_1^2 + a^4 \left(b^2 - (b^2 + a^2) \cos^2 \alpha \right) y_1^3 \\ q_3 &= b^4 \left(a^2 - c^2 \cos^2 \alpha \right) x_1^2 + a^4 \left(b^2 + c^2 \cos^2 \alpha \right) y_1^2 \\ &\quad + 2a^2 b^2 c^2 \cos \alpha \sin \alpha x_1 y_1. \end{aligned}$$

B.3. Caustic Semi-axes. In [6] the following explicit expressions were given for the axes of the Caustic:

$$(5) \quad a_c = \frac{a(\delta - b^2)}{c^2}, \quad b_c = \frac{b(a^2 - \delta)}{c^2}.$$

Two concentric, axis-aligned ellipses can generate a 3-periodic Poncelet family if and only if $a/a_c + b/b_c = 1$ [7], which holds above.

B.4. Joachimsthal's Invariant and Constant Orbit Perimeter. Joachimsthal's Integral implies that every trajectory segment is tangent to the Caustic [26]. Equivalently, a positive quantity γ remains invariant¹⁴ at every bounce point P_i :

$$(6) \quad \gamma = \frac{1}{2} \hat{v} \cdot \nabla f_i = \frac{1}{2} |\nabla f_i| \cos \alpha$$

where \hat{v} is the unit incoming (or outgoing) velocity vector, and:

$$\nabla f_i = 2 \left(\frac{x_i}{a^2}, \frac{y_i}{b^2} \right).$$

¹⁴The trajectory need not be periodic

Set $P_1 = (a, 0)$. An explicit expression for γ can be derived¹⁵ based on Equations (4) and (6):

$$(7) \quad \gamma = \frac{\sqrt{2\delta - a^2 - b^2}}{c^2}$$

Using the expressions for the vertices above, L can be computed explicitly:

$$L = 2(\delta + a^2 + b^2)\gamma$$

APPENDIX C. SEMIAXES OF THE ELLIPTIC LOCI

Table 1 lists the 29 of the first 100 Kimberling centers whose loci ellipses concentric and axis-aligned with the Billiard. Below we provide explicit expressions for the semi-axes a_i, b_i of said loci, i.e., let the locus of center X_i be described as:

$$(8) \quad \frac{x^2}{a_i^2} + \frac{y^2}{b_i^2} = 1$$

As above, $\delta = \sqrt{a^4 - a^2b^2 + b^4}$.

C.1. X_1 and Excenters.

$$a_1 = \frac{\delta - b^2}{a}, \quad b_1 = \frac{a^2 - \delta}{b}$$

The locus of the Excenters is an ellipse with axes:

$$a_e = \frac{b^2 + \delta}{a}, \quad b_e = \frac{a^2 + \delta}{b}$$

Notice it is similar to the X_1 locus, i.e., $a_1/b_1 = b_e/a_e$.

C.2. X_2 (similar to Billiard).

$$(a_2, b_2) = k_2(a, b), \text{ where } k_2 = \frac{2\delta - a^2 - b^2}{3c^2}$$

C.3. X_3 (similar to rotated Caustic).

$$a_3 = \frac{a^2 - \delta}{2a}, \quad b_3 = \frac{\delta - b^2}{2b}$$

Additionally, when $a/b = \frac{\sqrt{2\sqrt{33}+2}}{2} \simeq 1.836$, $b_3 = b$, i.e., the top and bottom vertices of the locus of X_3 coincide with the Billiard's.

¹⁵When $a = b$, $\gamma = \sqrt{3}/2$ and when $a/b \rightarrow \infty$, $\gamma \rightarrow 0$.

C.4. X_4 (similar to rotated Billiard).

$$(a_4, b_4) = \left(\frac{k_4}{a}, \frac{k_4}{b} \right), \quad k_4 = \frac{(a^2 + b^2)\delta - 2a^2b^2}{c^2}$$

Additionally:

- When $a/b = a_4 = \sqrt{2\sqrt{2}-1} \simeq 1.352$, $b_4 = b$, i.e., the top and bottom vertices of the locus of X_4 coincide with the Billiard's, Figure 9b.
- Let a_4^* be the positive root of $x^6 + x^4 - 4x^3 - x^2 - 1 = 0$, i.e., $a_4^* \simeq 1.51$. When $a/b = a_4^*$, $a_4 = b$ and $b_4 = a$, i.e., the locus of X_4 is identical to a rotated copy of Billiard, Figure 9c.

 C.5. X_5 .

$$a_5 = \frac{-w'_5(a, b) + w''_5(a, b)\delta}{w_5(a, b)}, \quad b_5 = \frac{w'_5(b, a) - w''_5(b, a)\delta}{w_5(b, a)}$$

$$w'_5(u, v) = u^2(u^2 + 3v^2), \quad w''_5(u, v) = 3u^2 + v^2, \quad w_5(u, v) = 4u(u^2 - v^2).$$

 C.6. X_7 (similar to Billiard).

$$(a_7, b_7) = k_7(a, b), \quad k_7 = \frac{2\delta - a^2 - b^2}{c^2}$$

 C.7. X_8 .

$$a_8 = \frac{(b^2 - \delta)^2}{ac^2}, \quad b_8 = \frac{(a^2 - \delta)^2}{bc^2}$$

 C.8. X_{10} (similar to rotated Billiard).

$$(a_{10}, b_{10}) = \left(\frac{k_{10}}{a}, \frac{k_{10}}{b} \right), \quad k_{10} = \frac{(a^2 + b^2)\delta - a^4 - b^4}{2c^2}$$

 C.9. X_{11} (identical to Caustic).

$$a_{11} = a_c, \quad b_{11} = b_c$$

 C.10. X_{12} .

$$a_{12} = \frac{-w'_{12}(a, b) + w''_{12}(a, b)\delta}{w_{12}(a, b)}, \quad b_{12} = \frac{w'_{12}(b, a) - w''_{12}(b, a)\delta}{w_{12}(b, a)}$$

$$w'_{12}(u, v) = v^2(15u^6 + 12v^2u^4 + 3u^2v^4 + 2v^6)$$

$$w''_{12}(u, v) = 7u^6 + 12v^2u^4 + 11u^2v^4 + 2v^6$$

$$w_{12}(u, v) = u(7u^6 + 11v^2u^4 - 11u^2v^4 - 7v^6).$$

 C.11. X_{20} .

$$a_{20} = \frac{a^2(3b^2 - a^2) - 2b^2\delta}{ac^2}, \quad b_{20} = \frac{b^2(b^2 - 3a^2) + 2a^2\delta}{bc^2}$$

C.12. X_{21} .

$$a_{21} = \frac{-w'_{21}(a, b) + w''_{21}(a, b)\delta}{w_{21}(a, b)}, \quad b_{21} = \frac{w'_{21}(b, a) - w''_{21}(b, a)\delta}{w_{21}(b, a)}$$

$$w'_{21}(u, v) = u^4 + u^2 v^2 + v^4, \quad w''_{21}(u, v) = 2(u^2 + v^2), \quad w_{21}(u, v) = u(3u^2 + 5v^2)$$

C.13. X_{35} .

$$a_{35} = \frac{-w'_{35}(a, b) + w''_{35}(a, b)\delta}{w_{35}(a, b)}, \quad b_{35} = \frac{-w'_{35}(b, a) + w''_{35}(b, a)\delta}{w_{35}(b, a)}$$

$$w'_{35}(u, v) = v^2(11u^4 + 4u^2v^2 + v^4), \quad w''_{35}(u, v) = (7u^2 + v^2)(u^2 + v^2)$$

$$w_{35}(u, v) = u(7u^4 + 18u^2v^2 + 7v^4)$$

C.14. X_{36} .

$$a_{36} = \frac{w'_{36}(a, b) + w''_{36}(a, b)\delta}{w_{36}(a, b)}, \quad b_{36} = \frac{-w'_{36}(b, a) - w''_{36}(b, a)\delta}{w(b, a)}$$

$$w'_{36}(u, v) = v^2(u^2 + v^2), \quad w''_{36}(u, v) = 3u^2 - v^2, \quad w_{36}(u, v) = 3u(u^2 - v^2)$$

C.15. X_{40} (similar to rotated Billiard).

$$a_{40} = \frac{c^2}{a}, \quad b_{40} = \frac{c^2}{b}$$

Additionally:

- When $a/b = \sqrt{2}$, $b_{40} = b$, i.e., the top and bottom vertices of the X_{40} locus coincides with the Billiard's.
- When $a/b = (1 + \sqrt{5})/2 = \phi \simeq 1.618$, $b_{40} = a$ and $a_{40} = b$, i.e., the X_{40} locus is identical to a rotated copy of Billiard.

C.16. X_{46} .

$$a_{46} = \frac{w'_{46}(a, b) + w''_{46}(a, b)\delta}{w_{46}(a, b)}, \quad b_{46} = \frac{-w'_{46}(b, a) - w''_{46}(b, a)\delta}{w_{46}(b, a)}$$

$$w'_{46}(u, v) = v^2(3u^2 - v^2)(u^2 - v^2), \quad w''_{46}(u, v) = (5u^2 + v^2)(u^2 - v^2)$$

$$w_{46}(u, v) = v(5u^4 - 6u^2v^2 + 5v^4)$$

C.17. X_{55} (similar to Caustic).

$$a_{55} = \frac{a(\delta - b^2)}{a^2 + b^2}, \quad b_{55} = \frac{b(a^2 - \delta)}{a^2 + b^2}$$

C.18. X_{56} .

$$a_{56} = \frac{-w'_{56}(a, b) + w''_{56}(a, b)\delta}{w_{56}(a, b)}, \quad b_{56} = \frac{w'_{56}(b, a) - w''_{56}(b, a)\delta}{w_{56}(b, a)}$$

$$\begin{aligned} w'_{56}(u, v) &= v^2(u^4 - u^2v^2 + 2v^4), & w''_{56}(u, v) &= 5u^4 - 5u^2v^2 + 2v^4 \\ w_{56}(u, v) &= u(5u^4 - 6u^2v^2 + 5v^4) \end{aligned}$$

C.19. X_{57} (similar to Billiard).

$$(a_{57}, b_{57}) = k_{57}(a, b), \quad k_{57} = \frac{c^2}{\delta}$$

C.20. X_{63} (similar to Billiard).

$$(a_{63}, b_{63}) = k_{63}(a, b), \quad k_{63} = \frac{c^2}{a^2 + b^2}$$

C.21. X_{65} .

$$a_{65} = \frac{w'_{65}(a, b) + w''_{65}(a, b)\delta}{w_{65}(a, b)}, \quad b_{65} = \frac{-w'_{65}(b, a) - w''_{65}(b, a)\delta}{w_{65}(b, a)}$$

$$\begin{aligned} w'_{65}(u, v) &= u^4v^2 + u^2v^4 + 2v^6, & w''_{65}(u, v) &= u^4 - 3u^2v^2 - 2v^4 \\ w_{65}(u, v) &= u(u^2 - v^2)^2 \end{aligned}$$

C.22. X_{72} .

$$a_{72} = \frac{w'_{72}(a, b) - w''_{72}(a, b)\delta}{w_{72}(a, b)}, \quad b_{72} = \frac{-w'_{72}(b, a) + w''_{72}(b, a)\delta}{w_{72}(b, a)}$$

$$w'_{72}(u, v) = u^6 + 2u^2v^4 + v^6, \quad w''_{72}(u, v) = (3u^2 + v^2)v^2, \quad w_{72}(u, v) = u(u^2 - v^2)^2$$

C.23. X_{78} .

$$a_{78} = \frac{w'_{78}(a, b) - w''_{78}(a, b)\delta}{w_{78}(a, b)}, \quad b_{78} = \frac{-w'_{78}(b, a) + w''_{78}(b, a)\delta}{w_{78}(b, a)}$$

$$\begin{aligned} w'_{78}(u, v) &= 5u^6 - 4u^4v^2 + u^2v^4 + 2v^6, & w''_{78}(u, v) &= 2v^2(u^2 + v^2) \\ w_{78}(u, v) &= u(5u^4 - 6v^2u^2 + 5v^4) \end{aligned}$$

C.24. X_{79} .

$$a_{79} = \frac{-w'_{79}(a, b) + w''_{79}(a, b)\delta}{w_{79}(a, b)}, \quad b_{79} = \frac{w'_{79}(b, a) - w''_{79}(b, a)\delta}{w_{79}(b, a)}$$

$$\begin{aligned} w'_{79}(u, v) &= v^2(11u^4 + 4v^2u^2 + v^4), & w''_{79}(u, v) &= (3u^4 + 12u^2v^2 + v^4) \\ w_{79}(u, v) &= u(u^2 - v^2)(3u^2 + 5v^2) \end{aligned}$$

C.25. X_{80} .

$$a_{80} = \frac{(\delta - b^2)(a^2 + b^2)}{ac^2}, \quad b_{80} = \frac{(a^2 - \delta)(a^2 + b^2)}{bc^2}$$

C.26. X_{84} (**similar to rotated Caustic**).

$$a_{84} = \frac{(b^2 + \delta)c^2}{a^3}, \quad b_{84} = \frac{(a^2 + \delta)c^2}{b^3}$$

C.27. X_{88} (**identical to Billiard**).

$$a_{88} = a, \quad b_{88} = b$$

C.28. X_{90} .

$$a_{90} = \frac{w'_{90}(a, b) + w''_{90}(a, b)\delta}{w_{90}(a, b)}, \quad b_{90} = \frac{w'_{90}(b, a) + w''_{90}(b, a)\delta}{w_{90}(b, a)}$$

$$\begin{aligned} w'_{90}(u, v) &= v^2(3u^2 - v^2)(u^2 - v^2), & w''_{90}(u, v) &= u^4 - v^4 \\ w_{90}(u, v) &= u(u^4 + 2u^2v^2 - 7v^4) \end{aligned}$$

C.29. X_{100} (**identical to Billiard**).

$$a_{100} = a, \quad b_{100} = b$$

APPENDIX D. ALGEBRAIC LOCUS

Here we provide expressions used in Section 4.

Let P_1, P_2, P_3 be an orbit's vertices. So sidelengths $s_1 = |P_3 - P_2|$, $s_2 = |P_1 - P_3|$, $s_3 = |P_2 - P_1|$. The following expressions are polynomials on s_i

and u, u_1, u_2 :

$$\begin{aligned}
g_1 &= -h_1 s_1^2 + h_0 \\
g_2 &= -h_1 s_2^2 - h_2 u_1 u_2 + h_3 \\
g_3 &= -h_1 s_3^2 + h_2 u_1 u_2 + h_3 \\
h_0 &= 12c^{12}(a^2 + b^2 + 2\delta)u^8 + 24c^{10}(a^2b^2 + 2b^4 - 2\delta c^2u^6 \\
&\quad - 4c^4[10a^{10} - 12a^8b^2 + 11a^6b^4 - 7a^4b^6 + 24a^2b^8 - 8b^{10} \\
&\quad - (2(4a^4 - 2a^2b^2 + b^4))(a^4 - 2a^2b^2 + 4b^4)\delta]u^4 \\
&\quad + 8a^6c^2[4a^6 - 7a^4b^2 + 11a^2b^4 - 2b^6 - (2(a^2 + ab + b^2))(a^2 - ab + b^2)\delta]u^2 + 4a^{12}\delta_1^2 \\
h_1 &= c^2(3c^4u^4 - 2c^2(a^2 - 2b^2u^2 - a^4))^2 \\
h_2 &= -2a(b^2 - \delta)\delta_1 u((3c^6\delta + (6(a^2 + b^2))c^6)u^6 + ((3(a^2 + 4b^2))c^4\delta \\
&\quad - (3(2a^4 - a^2b^2 - 4b^4))c^4)u^4 + ((b_2 - a^2)(7a^4 - 8b^4)\delta \\
&\quad + 2c^2(a^2 - 2b^2)(a^4 - 2b^4))u^2 + a^4(a^2 - 4b^2)\delta - a^4(2a^4 - 3a^2b^2 + 4b^4)) \\
h_3 &= c^6(9c^6u^{10} + 1)((18(a^4 + b^4))\delta - (3(7a^6 - 16a^4b^2 + 29a^2b^4 - 8b^6))u^8 \\
&\quad + 2c^2((13a^8 - 12a^6b^2 + 49a^4b^4 - 54a^2b^6 + 16b^8) - 2(10a^6 - 7a^4b^2 + 11a^2b^4 - 8b^6)\delta)u^6 \\
&\quad + ((28a^4\delta^2 - 40a^2b^6 + 16b^8)\delta - 26a^{10} + 12a^8b^2 + 42a^4b^6 - 48a^2b^8 + 16b^{10})u^4 \\
&\quad + a(13a^6 - 9a^4b^2 - 8b^4c^2 - (4(2a^4 + a^2b^2 - 2b^4))\delta)^4u^2 + 2a^8(\delta - a^8c^2) \\
\delta_1 &= \sqrt{2\delta - a^2 - b^2}
\end{aligned}$$

APPENDIX E. SYMMEDIAN LOCUS IS A QUARTIC

It can be shown that the locus X_6 is the quartic defined implicitly by:

$$\begin{aligned}
Q_4(x, y) &= b^4(5\delta^2 + 4(b^2 - a^2)\delta - a^2b^2)x^4 + a^4(5\delta^2 + 4(a^2 - b^2)\delta - a^2b^2)y^4 \\
&\quad + 2a^2b^2(a^2b^2 + 3\delta^2)x^2y^2 + a^2b^4(3b^4 + 2(2a^2 - b^2)\delta - 5\delta^2)x^2 \\
&\quad + a^4b^2(3a^4 + 2(2b^2 - a^2)\delta - 5\delta^2)y^2
\end{aligned}$$

One can also calculate an axis-aligned ellipse with semi-axes:

$$a_6 = \frac{(-(a^2 + b^2)b^2 + (3a^2 - b^2)\delta)a}{a^4 + b^4 + 2\delta^2}, \quad b_6 = \frac{(a^2(a^2 + b^2) + (a^2 - 3b^2)\delta)b}{a^4 + b^4 + 2\delta^2}$$

which is internally tangent to $Q_4(x, y) = 0$ at its four vertices.

DAN REZNIK, DATA SCIENCE CONSULTING, RIO DE JANEIRO, RJ, BRAZIL

E-mail address: `dan@dat-sci.com`

RONALDO GARCIA, INST. DE MATEMÁTICA E ESTATÍSTICA, UNIV. FEDERAL DE
GOIÁS, GOIÂNIA, GO, BRAZIL

E-mail address: `rgarcia@ufg.br`

JAIR KOILLER, DEPT. DE MATEMÁTICA, UNIV. FEDERAL DE JUIZ DE FORA, JUIZ
DE FORA, MG, BRAZIL

E-mail address: `jairkoiller@gmail.com`